

AD-A075 131

NAVAL OCEAN SYSTEMS CENTER SAN DIEGO CA

F/G 17/1

PHASE INTEGRAL ALGORITHMS FOR SIGNAL SPEEDS IN RANGE-DEPENDENT --ETC(U)

JUL 78 R C SHOCKLEY

UNCLASSIFIED

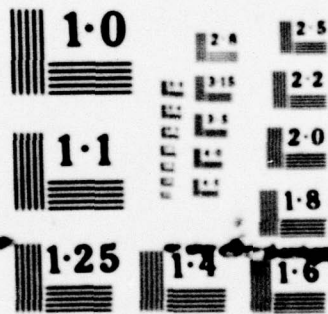
NOSC/TR-412

NL

1 OF 1  
AD-A075131

NOSC





NATIONAL BUREAU OF STANDARDS  
MICROCOPY RESOLUTION TEST CHART

AD A075131

NOSC TR 412

12  
**NOSC**

**LEVEL** II

NOSC TR 412

**Technical Report 412**

**PHASE INTEGRAL ALGORITHMS FOR  
SIGNAL SPEEDS IN RANGE-DEPENDENT  
SOUND VELOCITY PROFILES**

**R. C. Shockley**

**10 July 1978**

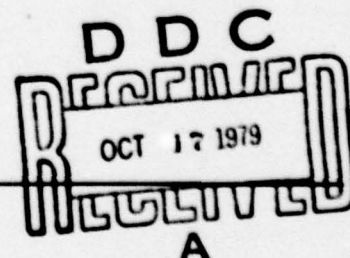
**Final Report: January 1978 — July 1978**

**Prepared for  
Naval Electronic Systems Command  
(PME 124)**

**DDC FILE COPY**

Approved for public release; distribution unlimited

**NAVAL OCEAN SYSTEMS CENTER  
SAN DIEGO, CALIFORNIA 92152**



79 10 17 069



NAVAL OCEAN SYSTEMS CENTER, SAN DIEGO, CA 92162

---

**AN ACTIVITY OF THE NAVAL MATERIAL COMMAND**

**RR GAVAZZI, CAPT, USN**

*Commander*

**HL BLOOD**

*Technical Director*

**ADMINISTRATIVE INFORMATION**

This work pertains to a method for estimating from archival sound speed profile data the effective signal speed in range-dependent environments. The method employs the adiabatic invariance of the phase integral for underwater sound rays, and offers certain computational advantages in the context of improved time-difference-of-arrival performance using Multi-Array Correlation (MAC) equipment. The work was done under NOSC 24311N, X0522114, and was sponsored by Naval Electronic Systems Command (PME-124).

Released by  
M. R. Akers, Head  
System Concepts and Analysis Division

Under Authority of  
E. B. Tunstall, Head  
Ocean Surveillance Department



UNCLASSIFIED

SECURITY CLASSIFICATION OF THIS PAGE (When Data Entered)

REPORT DOCUMENTATION PAGE		READ INSTRUCTIONS BEFORE COMPLETING FORM
1. REPORT NUMBER Technical Report 412 (TR 412)	2. GOVT ACCESSION NO. 14	3. RECIPIENT'S CATALOG NUMBER NSEC/TR-412
4. TITLE (and Subtitle) PHASE INTEGRAL ALGORITHMS FOR SIGNAL SPEEDS IN RANGE-DEPENDENT SOUND VELOCITY PROFILES		5. TYPE OF REPORT & PERIOD COVERED Final Report, Jan 1977 - Jul 1978
7. AUTHOR(s) R. C. Shockley		6. PERFORMING ORG. REPORT NUMBER
9. PERFORMING ORGANIZATION NAME AND ADDRESS Naval Ocean Systems Center San Diego, CA 92110		8. CONTRACT OR GRANT NUMBER(s)
11. CONTROLLING OFFICE NAME AND ADDRESS Naval Electronic Systems Command Washington, DC 20360		10. PROGRAM ELEMENT, PROJECT, TASK AREA & WORK UNIT NUMBERS 24311N XO522114
14. MONITORING AGENCY NAME & ADDRESS (if different from Controlling Office)		12. REPORT DATE 18 July 1978
		13. NUMBER OF PAGES 47
		15. SECURITY CLASS. (of this report) Unclassified
		15a. DECLASSIFICATION/DOWNGRADING SCHEDULE
16. DISTRIBUTION STATEMENT (of this Report)  Approved for public release; distribution unlimited.		
17. DISTRIBUTION STATEMENT (of the abstract entered in Block 20, if different from Report)		
18. SUPPLEMENTARY NOTES		
19. KEY WORDS (Continue on reverse side if necessary and identify by block number) Adiabatic invariant                      Sound speed algorithms Guided propagation                      Underwater sound Range dependent profiles SOFAR		
20. ABSTRACT (Continue on reverse side if necessary and identify by block number) The adiabatic invariance of the phase integral $J = \oint \sin \theta \, dz/c$ for ducted sound rays in SOFAR channels is demonstrated by means of exact raytracing solutions in range-dependent channels. FORTRAN algorithms for this and for relating $J$ to the average ray speed in arbitrary ducts are presented and discussed in the context of acoustic surveillance.		

DD FORM 1 JAN 73 1473

EDITION OF 1 NOV 68 IS OBSOLETE  
S/N 0102-LF-014-6601

UNCLASSIFIED

SECURITY CLASSIFICATION OF THIS PAGE (When Data Entered)

393 159

## FOREWORD

↙ This report presents two Fortran raytracing codes and related theory which are designed to treat underwater sound propagation in the presence of range-dependent sound velocity profiles (SVPs). Particular emphasis is placed on the average horizontal ray velocity and its variation as a ray traverses different SVPs. Efficient calculation of this variation is of great importance for improved modern multisensor localization techniques. The following pages discuss the adiabatic invariant approximation (AIA) and the use of the codes RAY1 and RAY2 in sufficient depth that the reader may apply them to his own problems or modify them for this purpose. This work was supported by the Naval Electronic Systems Command PME-124 under the Performance Evaluation and Prediction program at the Naval Ocean Systems Center. Portions of this work have appeared in the Journal of the Acoustical Society of America.

## OBJECTIVE

The objective of the work was to calculate efficiently the variation of the average horizontal ray velocity as the ray traverses different sound velocity profiles. Efficient calculation of this variation is of great importance for improved modern multisensor localization techniques.

## RESULTS

↙ The adiabatic invariant approximation agrees well with exact raytracing results even for strongly inhomogeneous sound velocity profiles. Simple algorithms are developed for demonstrating this and for computing the adiabatic invariant in arbitrary profiles for a user-selected family of rays. ↙

## RECOMMENDATIONS

A set of curves or tables should be prepared showing the functional relation between the adiabatic invariant, the average sound speed, and the ray angle, for areas of high interest in acoustic surveillance. These would provide a data base for improved multisensor localization and would reduce the calculation of average ray speeds to a table-look-up procedure once the location of the source is known approximately.

Accession For	
NTIS GRA&I	<input checked="checked" type="checkbox"/>
DDC TAB	<input type="checkbox"/>
Unannounced	<input type="checkbox"/>
Justification	
By _____	
Distribution/	
Availability Codes	
Disc	Avail and/or special
A	

## CONTENTS

I. INTRODUCTION . . .	page 3
II. GENERAL DESCRIPTION OF RAY1 AND RAY2 . . .	4
A. The Adiabatic Invariant for Sound Rays . . .	4
B. General Description of RAY1 . . .	8
C. General Description of RAY2 . . .	12
III. INSTRUCTIONS FOR USING RAY1 . . .	15
A. Input Requirements . . .	15
B. Output . . .	15
IV. INSTRUCTIONS FOR USING RAY2 . . .	17
A. Input Parameter List . . .	17
B. Output . . .	18
V. INTERNAL LOGICAL STRUCTURE OF RAY1 AND RAY2 . . .	20
A. Internal Structure of RAY1 . . .	20
B. Internal Structure of RAY2 . . .	22
VI. LISTINGS OF RAY1 AND RAY2 . . .	24
REFERENCES . . .	47



## I. INTRODUCTION

Several important problems in underwater sound, ionospheric propagation, and seismic research involve the presence of ducts or waveguides which effectively trap the energy, greatly reducing transmission loss over the corresponding case of an isotropic medium. Often, however, the duct varies with range, precluding exact normal mode solutions and affecting signal speeds in a generally complicated fashion. The range variation may consist of changes in the physical dimensions of the duct or in the index of refraction across the duct.

Simple computational methods are desired for estimating the influence of such range-dependence. The requirements basically are that the procedure be readily checked against known exact solutions, that it be relatively inexpensive to implement using archival data bases, and that revisions of the data should be readily incorporated in the method, without requiring massive recomputation.

An attractive candidate for meeting these needs is the adiabatic invariant approximation (AIA). This presupposes that in the cases of interest any range-dependent variations take place over distances large compared to a single ray cycle. In other words, the properties of the medium should be sensibly constant over a cycle. Under such conditions, which nearly always apply for deep sound channels, it turns out that ray paths evolve in range so as to keep a certain quantity ( $J$ ) constant, known as the action integral or phase integral.<sup>1</sup> This "conservation law" allows one to follow a ray, in essence, without ever tracing it over its entire path. It is only necessary to know in each local region how the quantities of interest (eg. maximum depth of the ray, vertexing speed, average horizontal velocity, etc.) are related to the adiabatic invariant  $J$ , something easily done simply by tracing a few ray cycles in each local region.

Although we have been speaking in terms of rays, adiabatic invariants appear in mode theory as well. Each mode corresponds to a particular vertexing depth and speed for the associated family of rays. In referring only to rays, as we shall do throughout what follows, we are assuming the duct supports so many modes that they comprise a continuum in effect; their discrete nature may be disregarded without significant loss of accuracy. Since deep sound channels are of the order of ten or more wavelengths across at frequencies of interest for time difference fixing, the mode-continuum approximation is generally quite good. The low order modes are not strongly excited by acoustic sources, which are usually far from the sound channel axis.

When one has only low order modes, the adiabatic invariants are the mode numbers themselves. This is intuitively plausible, for if one considers an arbitrarily gradual evolution of one duct into a second one, having, say, a somewhat different index profile, then it is clear that the power initially in a particular mode must equal the power in that mode in the altered duct. Only rather strong perturbations will cause mode coupling; in their absence, there is no cause for energy to distribute itself among any other discrete modes.

---

1. Weston, DE, *Guided Propagation in a Slowly Varying Medium*, Proc. Phys. Soc. (London) v. 73, p. 365-384, 1958.

Exceptions to this simple picture obviously exist in cases where one duct evolves into two. In such cases one cannot treat the splitting of acoustic energy accurately unless the details of the SVP evolution are considered. Fortunately, such cases are rare. The procedures described in this report should be applicable to all ocean areas of surveillance interest.

The computer codes described here serve two purposes. RAY1 allows one to set up a radically inhomogeneous medium whose SVP has a prescribed functional form and to determine numerically by how much the approximation  $J = \text{constant}$  fails for various horizontal gradients. RAY2 allows one to input an arbitrary but range-independent SVP and to trace a family of rays in order to find the relation between  $J$  and other properties of interest for rays in that particular SVP. The former code is of primarily theoretical interest, and serves to establish the accuracy for the AIA in analytically tractable cases, while it is our hope that the latter will serve as a model for implementation of AIA methods in acoustic surveillance.

In section II we describe in general terms the scope of RAY1 and RAY2, we review briefly the adiabatic invariant theory as applied to acoustic rays, the analogous problem in classical mechanics, and finally give the AIA signal speed algorithm. Sections III and IV provide instructions in detail on the procedure for executing RAY1 and RAY2. In section V, we shall treat the internal logical structure of RAY1 and RAY2 in order to pave the way for any changes deemed necessary or desirable. Listings of the Fortran source code appear in section VI.

## II. GENERAL DESCRIPTION OF RAY1 AND RAY2

In this section we shall describe the general features of RAY1 and RAY2 and the theory behind these codes. In sections III and IV we shall present specific information needed to make runs with these codes. Here we are concerned with the practical need for such codes, and the underlying concept of using an adiabatic invariant as a means for following the evolution of rays in range-dependent SVPs.

### A. THE ADIABATIC INVARIANT FOR SOUND RAYS

The basic problem of time-difference fixing provides a context for introducing the adiabatic invariant concept. For simplicity, suppose that acoustic signals propagate with the same speed in the ocean regardless of direction. In this isotropic ocean, a pair of sensors which receive a given signal may determine, based on the difference of arrival times, a locus of points on which the source must lie. The locus is a hyperbola with the sensors as foci. If  $R_1$  and  $R_2$  represent distances to sensors 1 and 2 respectively, and  $c\Delta t$  represents the equivalent delay length, then  $|R_1 - R_2| = c\Delta t$  determines the hyperbola. A third sensor, or some additional data from one of the original two, then suffices to locate the source uniquely. (Ambiguities arising in particular geometries are not of interest here, although they may be important in practice.)

The procedure just described works only approximately in actual ocean environments. For long-range detections on the order of several hundred kilometers the signal speed generally will vary with range. Modern acoustic surveillance systems are capable of sufficiently precise measurement that this inhomogeneity poses a major limitation on localization. How can one determine an appropriate average sound speed so as to construct the needed locus?



A natural solution is to use a conserved quantity for sound rays in range-dependent environments. Weston<sup>1</sup> has pointed out that the quantity

$$J = \oint c^{-1} \sin \theta \, dz \quad (1)$$

is conserved provided that changes in the SVP are sufficiently gradual, or "adiabatic." Here  $c$  is the local depth-dependent sound speed, and is regarded as being range-independent over the period of integration (one ray cycle),  $\theta$  is the ray angle measured with respect to horizontal, and  $z$  is the depth coordinate (usually taken as positive downwards). More detailed discussion of the invariance of  $J$  in range-dependent SVPs, as well as a short bibliography on the topic, will be found in reference 2. A proof of the adiabatic invariance of the action integral will be found in reference 3. At this point it may be of interest to consider the mechanical analogue of trapped sound rays and eq (1).

### 1. Classical Mechanical Analogy

Ray theory is of course an approximation to an "exact" wave theory of propagation. In the same sense, classical mechanics is an approximation to the more precise quantum mechanical theory. In both cases the smallness of the wavelength with respect to the physical dimensions of the medium or measuring apparatus involved permits one to pass over to the geometrical optics limit, ignoring small wavelength-dependent corrections. In classical mechanics, the motion of a system is obtainable from Hamilton's principle, which is a variational principle, stating that the actual trajectory followed is such as to minimize the integral  $\int_{t_1}^{t_2} L(\dot{q}, q; t) \, dt$ . (Actually the statement of Hamilton's principle permits

maximization as well, but we shall not be concerned with this in what follows.) Here  $L$  is the Lagrangian, a function of the coordinates and velocities, symbolically denoted  $q$  and  $\dot{q}$ , respectively, and possibly of time  $t$ . The coordinates and velocities are functions of time. The system moves from some fixed starting point  $(q(t_1), \dot{q}(t_1))$  to a final point  $(q(t_2), \dot{q}(t_2))$ , also fixed. Hamilton's principle is written

$$\delta \int_{t_1}^{t_2} L \, dt = 0 \quad (2)$$

where  $\delta$  indicates an infinitesimal variation of the path. Equation (2) states that the system follows a minimizing trajectory, since any infinitesimal variation about the trajectory must produce no change in the value of the integral.

In classical mechanics, the equations of motion follow if one uses for the Lagrangian  $L = T - V$ , where  $T$  is the kinetic energy and  $V$  the potential energy of the system. Then the calculus of variations yields, as a theorem from eq (2), Newton's equation of motion.

2. Shockley, RC, *Paraxial and Nonparaxial Ray Speeds in Strongly Range-Dependent SOFAR Channels*, J. Acoust. Soc. Am. v. 64, p. 1171-1177 (1978).

3. Landau, LD and Lifshitz, EM, *Mechanics*, Pergamon Press, Reading, Mass., p. 154-158, 1960.

Variational principles (with different choices for  $L$ ) also lead to the equations of electrodynamics, hydrodynamics, quantum mechanics, etc., in similar fashion.

If we consider Fermat's principle, the similarity to Hamilton's principle is clear. Fermat's principle states that a ray will follow that trajectory minimizing the time of flight between a given initial and final point:

$$\delta \int_1^2 dt = \delta \int_1^2 ds/c = 0 \quad (3)$$

where  $ds$  is an infinitesimal element of length along the ray path and  $c$  the speed of propagation in the medium.

For concreteness, we restrict our discussion to a slab symmetric medium and let  $x$  be the horizontal and  $z$  the vertical coordinate. Then eq (3) becomes

$$\delta \int_1^2 c^{-1} (1 + \dot{z}^2)^{1/2} dx = 0 \quad (4)$$

where  $\dot{z} \equiv dz/dx$  is the slope of the ray. This result now is identical to eq (2), Hamilton's principle, under the transformation

$$\begin{aligned} t &\rightarrow x, \\ q &\rightarrow z, \\ L(q, \dot{q}; t) &\rightarrow (1 + \dot{z}^2)^{1/2}/c(z; x) \end{aligned} \quad (5)$$

Thus range plays the role of time in the mechanical problem, and the depth  $z$  is analogous to particle displacement. Hence  $\dot{z} = \tan\theta$  is analogous to velocity. Note that  $L$  does not resemble a quantity like  $T-V$ .

It is natural to ask what equation involving the "acceleration"  $\ddot{z}$  is analogous to Newton's equation of motion. The answer provides insight into the behavior of rays in deep sound channels and bears directly on the raytracing routine employed in RAY1 and RAY2. The Euler-Lagrange equation, which follows as a theorem<sup>3</sup> from the variational principle in eq (2), as mentioned above, states that

$$(d/dt) \partial L / \partial \dot{q} - \partial L / \partial q = 0 \quad (6)$$

If the reader applies the transformation given in eq (5) then, after some algebraic manipulation, eq (6) will be seen to become

$$\ddot{z} = -(1 + \dot{z}^2) c^{-1} \partial c / \partial z + \dot{z} (1 + \dot{z}^2) c^{-1} \partial c / \partial x \quad (7)$$

a result obtained previously by Milder.<sup>2,4</sup> Equation (7) is similar to Newton's equation of motion, giving the acceleration as a function of displacement, velocity, and time.

RAY1 and RAY2 use a fourth order Runge-Kutta scheme<sup>2</sup> to integrate eq (7), and thus obtain the ray depth as a function of range. Equation (7) describes the ray

4. Milder DM, *Ray and Wave Invariants for SOFAR Channel Propagation*, J. Acoust. Soc. Am., v. 46, p. 1259-1263 (1969).



curvature in terms of the local sound speed derivatives in depth and range and the ray slope. For prescribed initial conditions  $z(0)$  and  $\dot{z}(0)$ , and a given function  $c(z; x)$ , it specifies a unique trajectory satisfying Fermat's principle.

When the medium is range-independent, the second term on the right-hand side of eq (7) vanishes. A further simplification comes about since in range-independent media Snell's law holds in the form  $c_v = c/\cos\theta$ , where  $c_v$  is the constant vertexing speed (where  $\dot{z} = 0$ ). Thus eq (7) becomes

$$\ddot{z} = -c_v^2 (dc/dz) c^{-3} = -(\partial/\partial z) (-c_v^2/2c^2) \quad (8)$$

Hence in range-independent SVPs the motion of a ray is precisely analogous to the trajectory of a mechanical particle of unit mass under the action of a potential field given by

$$V(z) = -c_v^2/2c^2 \quad (9)$$

This result allows considerable insight into the trajectories of rays. For example, if we consider the Hirsch profile

$$c(z) = c_0/(1 - z^2/a^2)^{1/2}$$

then the potential is

$$\begin{aligned} V(z) &= -(c_v/c_0)^2 (1 - z^2/a^2) \\ &= (c_v/c_0 a)^2 z^2 + \text{const} \end{aligned}$$

which is a quadratic function of  $z$ , the same as a simple harmonic oscillator. Ray paths must therefore be sine waves in this SVP. It is simple to sketch potential functions for any reasonable SVP, and range-dependence may be included in this analogy by allowing  $V(z)$  to vary slowly with time.

When the medium is range-dependent, then the analogous classical mechanics problem involves a time-dependent potential, as one can see from the transformation eq (5). Hence the energy of the analogous particle is not conserved, nor are the positions of the turning points where  $\dot{q} = 0$  or  $\dot{z} = 0$ . If the variations are gradual, however, the action integral

$$J = \oint p dq \quad (10)$$

is approximately conserved.<sup>3</sup> Here  $p \equiv \partial L/\partial \dot{q}$ ;  $p$  is called the momentum canonically conjugate to the coordinate  $q$  in classical mechanics. If the reader again applies eq (5) and uses  $\dot{z} = \tan\theta$ , he will find

$$p = \dot{z}/c (1 + \dot{z}^2)^{1/2} = \sin\theta/c$$

and thus eq (1) follows as the adiabatic invariant for sound rays. Note that the integral covers one cycle of the trajectory and represents the area of an (almost) closed loop traced

out in p-q space, known as phase space. The path is a closed loop for range-independent SVPs.

## 2. AIA Algorithm for Average Horizontal Ray Velocity

One may use the invariance of  $J$  to compute the average horizontal velocity of a ray traversing a range-dependent SVP as follows. We assume it is possible to break up the entire region of interest into local regions bounded by some set of contiguous contours inside each of which  $c(z)$  is a known function, which can be regarded as range-independent within the local region.

First one constructs tables showing the relationship between  $J$  and  $\bar{c}$ , the average horizontal ray velocity, for each local region. This may require tracing perhaps 10 to 50 rays for each SVP. Each ray need only be traced for a small number of cycles (one or two) to find  $J$  and  $\bar{c}$  for the given initial conditions. These tables then allow one to find how  $\bar{c}$  varies from region to region for a particular  $J$  value, by employing simple table-look-up procedures.

This method does not yield detailed information on the trajectory, such as positions of ray turning points in range, but this is the cost of obtaining estimates of  $\bar{c}$  for long-range paths with simple algorithms. For a prescribed path, one then may find the effective signal speed for given initial conditions (depth and ray angle) from the  $\bar{c}$  values in each region according to the fraction of time spent in each region. If  $R$  denotes the total range,  $R_i$  the distance traveled in region  $i$ , and  $\bar{c}_i$  the average horizontal velocity in region  $i$ , then the effective signal speed is given by

$$\bar{c} = R / \sum_i (R_i / \bar{c}_i) \quad (11)$$

Additional algorithms are necessary to select a range of initial conditions that characterize rays which carry most of the acoustic energy. Depending on the geometry, these may range from simple inspection procedures to complicated ray-trace routines requiring detailed bathymetry charts. Reference 2 discusses possible methods for selecting appropriate ranges of  $J$  values using the output of RAY2 (see section VI). Further remarks on this are included in section IIC, where we indicate how certain of the quantities computed by RAY2 facilitate ray selection.

## B. GENERAL DESCRIPTION OF RAY1

A listing of the code RAY1 will be found in section V, and instructions on its use in section III. Here we shall describe the general features of RAY1.

RAY1 provides quantitative answers to the question of the validity of the AIA. Earlier we noted that  $J$  is conserved for sufficiently slow variations in the SVP. More precisely,  $J$  is conserved (or nearly so) provided that any changes in the SVP are fractionally small over one cycle distance (in range) of the ray. This follows from the fundamental law of ray theory, Fermat's principle of least time<sup>3</sup> as discussed in section II.A.1. We refer the reader desiring further discussion of this to Landau and Lifshitz<sup>3</sup> and the bibliography of reference 2.

In real ocean environments, the adiabatic condition is satisfied for RR (Refracted Refracted) rays, but one still may ask what degree of inhomogeneity is required before the AIA fails badly. RAY1 provides specific answers to this by allowing the user to control the horizontal gradients of parameters in the SVP function. Thus both the degree of inhomogeneity and the effect of the functional form  $c(z)$  may be investigated.

Presently three self-similar SVPs are available as subroutines in RAY1. They are the parabolic profile,

$$c(z, x) = c_0(z) [1 + z^2/a^2(x)] \quad , \quad (12a)$$

the Hirsch profile,

$$c(z, x) = c_0(z) [1 - z^2/a^2(x)]^{-1/2} \quad , \quad (12b)$$

and the bilinear profile,

$$c(z, x) = c_0(x) [1 \pm z/a(x)] \quad , \quad z > 0 (< 0) \quad (12c)$$

Figure 1 shows these SVPs for range-independent SVPs. Each of equations (3) describes a slab symmetric (depending only on range  $x$  and depth  $z$ ) sound channel with an axis at  $z = 0$ , and an axial sound speed  $c_0(x)$ . Both  $c_0(x)$  and  $a(x)$  are linear functions of  $x$  in the current version of RAY1. By varying their derivatives with appropriate input data, the user may study the degree to which nonadiabatic changes in the SVP affect the action integral, or the discrepancy between the computed average horizontal ray velocity and the predicted value, assuming  $\partial J/\partial x = 0$ . Details on the program inputs will be deferred until section III.

RAY1 allows the user to select one of the three SVPs, and control tracing of rays in the presence of constricting (if  $da/dx < 0$ ) or widening ( $da/dx > 0$ ) sound channels. Gradients in  $c_0$  and  $a$  are independent. In addition, the raytracing routine employed (a fourth order Runge-Kutta algorithm applied to the Euler-Lagrange equation of motion obtained from Fermat's principle) has an automatic test and redefinition routine which refines the step size  $dx$  when there are fewer than 150 steps per half-cycle, although this number can be easily modified (see section V).

For completeness, we present in table 1 the analytic formulae for ray paths and the average horizontal ray velocity in each of the SVPs in RAY1 for range-independent conditions. For the parabolic SVP,  $u_1$  and  $E(u_1)$  are the normal elliptic integrals of the first and second kind, respectively, with argument  $z/a$ , modulus squared  $(\alpha-1)^2/2(\alpha^2+1)$  where  $\alpha^2 \equiv c_v/c_0$ ;  $\text{sn } u_1$ ,  $\text{cn } u_1$  and  $\text{dn } u_1$  are Jacobian elliptic functions;  $E(k)$ ,  $K(k)$  and  $\Pi(\beta^2, k)$  are complete elliptic integrals of the first, second, and third kind with  $k^2 = (\alpha-1)^2/(2\alpha^2+2)$  and the parameter  $\beta^2 = (1-\cos\theta_0)/2$ .<sup>5</sup>  $\theta_0$  is the angle with respect to horizontal at which the ray crosses the sound channel axis at  $z = 0$  in all formulae.

Figures 2 and 3 show the agreement found for  $\theta_0(0) = 30^\circ$  in an earlier study<sup>2</sup> between predicted sound speeds, assuming  $\partial J/\partial x = 0$ , and those computed by RAY1 in the

5. Byrd, PF and Friedman, MD, *Handbook of Elliptic Integrals for Engineers and Scientists*, Springer Verlag, New York (1971).



presence of various gradients in  $a(x)$ , the depth scaling function. The agreement generally is good even when the environment changes rapidly, for example by 40% (in  $a(x)$ ) in a single ray cycle. Such agreement, although it cannot be expected for all SVP choices, lends considerable support to the general validity of the AIA. Quantitative answers to this question are of interest since the AIA method seems to offer a simple solution to some time difference fixing (TDF) problems: data bases for implementing AIA sound speed algorithms are easily generated, the table-look-up AIA computations typically are far less time-consuming than long-range raytracing, and the method permits very flexible updating of data in individual SVP regions without requiring long-range raytracing computations to be repeated.

In figures 2 and 3  $x_p$  is the cycle distance and  $x_c$  the critical range at which the channel constricts to an extent such that rays are reflected, and cannot propagate further. The notation  $x_c/x_p$  ( $x=0$ ) is the ratio of the critical range to a cycle distance, evaluated at the initial range. Thus, for example, if  $x_c/x_p = 3$ , the critical constriction occurs only 3 cycle distances from the ray's starting point. The vertical axis is the normalized average horizontal ray speed ( $\bar{c}^* = 1$  for a ray on the channel axis) and the horizontal axis is the normalized channel width parameter ( $a^* = a/a_0$  where  $a$  is the scale length in the table 1 formulas, and  $a_0$  is the initial value of  $a$ ).

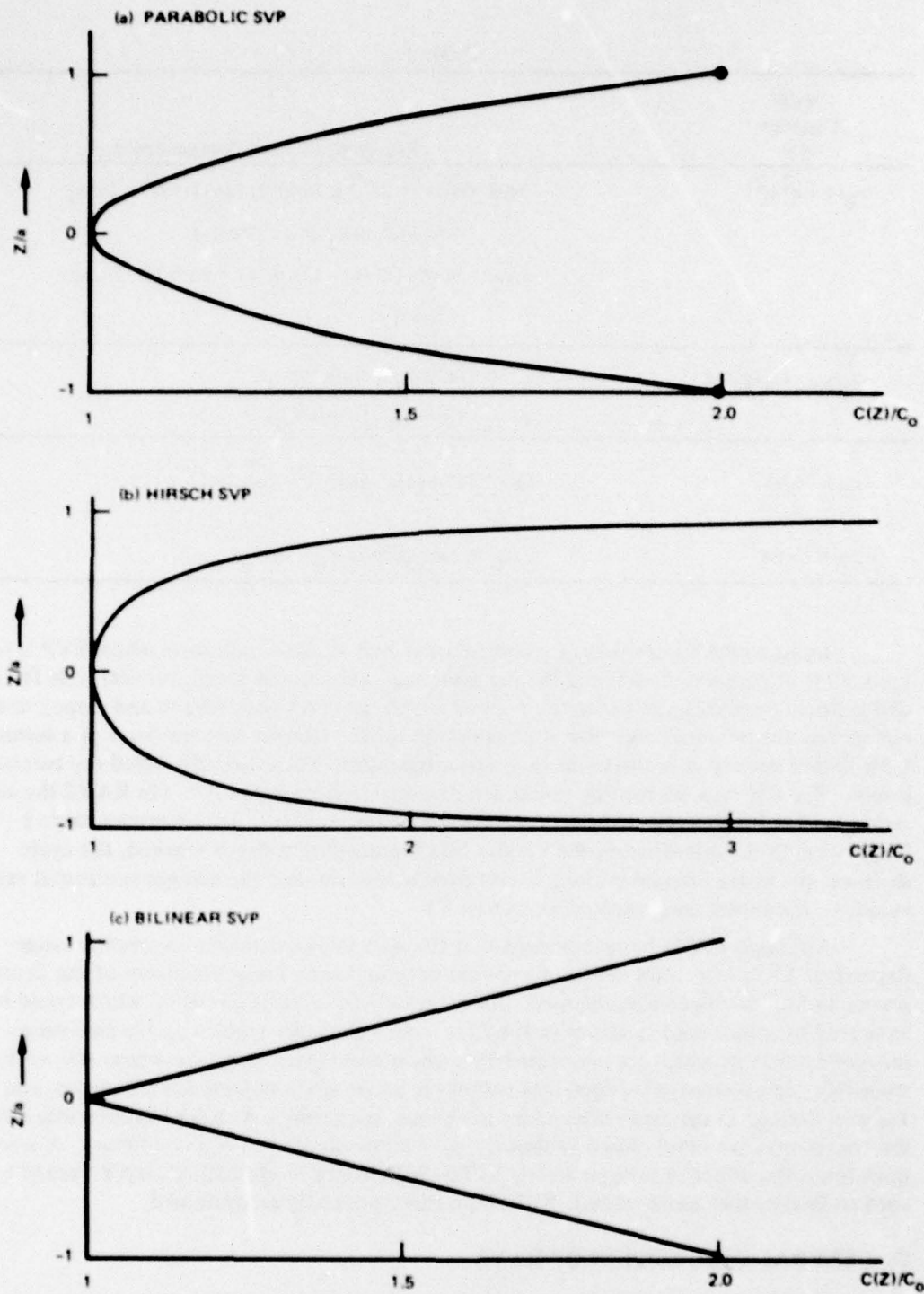


Figure 1. Three analytical forms for model sound velocity profiles (from eq (12)) in dimensionless form.

Table 1.

SVP Function $c(z)$	Ray Trajectory and Average Speed
$c_0(1 + z^2/a^2)$	$x/a = (2\alpha^2 + 2)^{-1/2} [(2\alpha^2 + 2) E(u_1) - (\alpha^2 + 2\alpha)u_1 - (\alpha - 1)^2 \operatorname{sn} u_1 \operatorname{cn} u_1 / \operatorname{dn} u_1]$ $\bar{c}/c_0 = \sec\theta_0 (2E(k) - K(k)) / [(1 + \sec\theta_0) \Pi(\beta^2, k) - K(k)]$
$c_0(1 - z^2/a^2)^{-1/2}$	$z = a \sin\theta_0 \cos(x/a \cos\theta_0)$ $\bar{c}/c_0 = 2 \cos\theta_0 / (1 + \cos^2\theta_0)$
$c_0(1 \mp z/a)$	$(z/a + 1)^2 + (x/a - \tan\theta_0)^2 = \sec^2\theta_0$
$z < 0 (> 0)$	$\bar{c}/c_0 = \tan\theta_0 / \operatorname{kn}(\sec\theta_0 + \tan\theta_0)$

Input to RAY1 consists of a control or switch variable indicating which SVP is to be used, a set of parameters defining the medium (e.g., axial sound speed, vertical scale factor, and gradients with respect to range), a set of initial ray conditions (depth and slope), and parameters for the range step size and maximum range. Output is in the form of a summary table listing the ray coordinates at each vertexing point. These are also called ray turning points. For RR rays, all turning points are characterized by  $dz/dx = 0$ . (In RAY2 the surface reflection for RSR (Refracted-Surface-Reflected) rays leads to a discontinuous slope.) In addition to the coordinates, RAY1 also lists the maximum depth reached, the cycle distance, the phase integral evaluated over each half-cycle, and the average horizontal ray velocity. Examples are presented in section VI.

Although RAY1 has established that the AIA works well even in severely range-dependent SVPs of certain kinds, one should note that only linear variations of the depth scaling factor have been programmed. An extremely interesting question, which could be answered by minor modifications in RAY1, involves the conservation of  $J$  in two range-independent SVPs which are connected by some inhomogeneous region where  $a(x)$  varies smoothly. In each range-independent region the phase space trajectories are closed, and  $J$  is well defined as the area enclosed by the phase space orbit. As RAY1 is currently written, the trajectories are never closed (unless the user inputs  $da/dx = 0$  as a condition). A second question is the effect of nonsymmetric SVPs. With minor modifications, RAY1 could be used to study other more realistic SVPs than those presently programmed.

### C. GENERAL DESCRIPTION OF RAY2

RAY2 consists of four Fortran routines which trace a family of rays in a user supplied SVP, computing for each ray the turning point coordinates (depth, range, and time), the



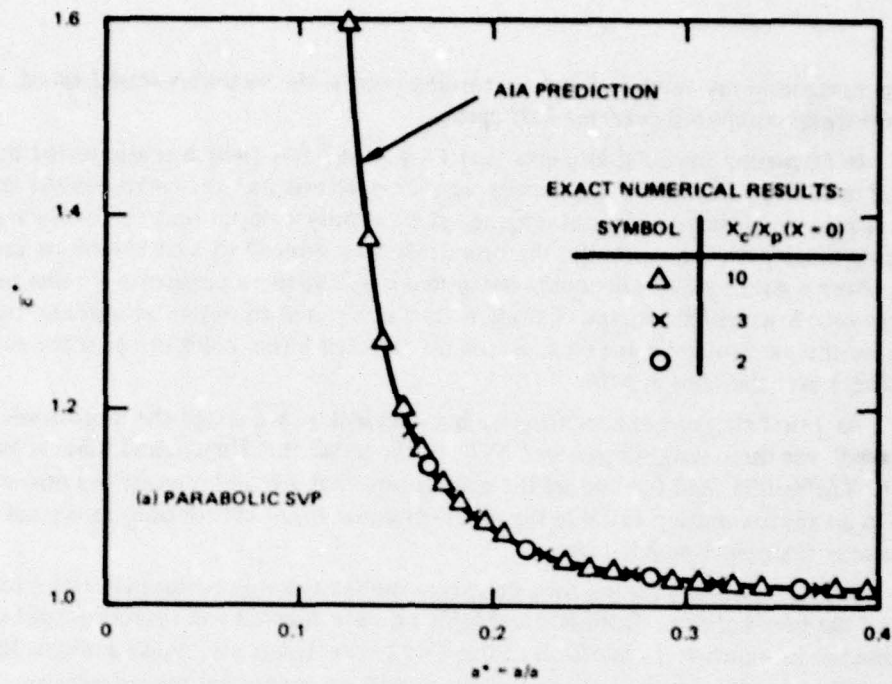


Figure 2. Comparison of AIA predictions and exact numerical results for parabolic SVP (from ref. 2).

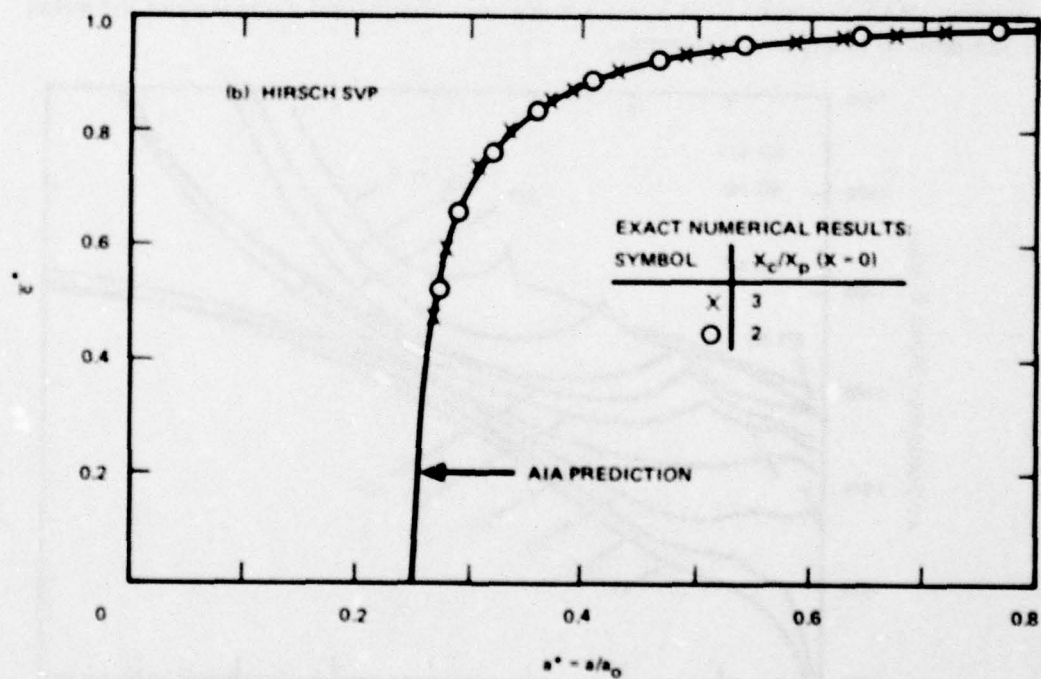


Figure 3. Comparison of AIA predictions and exact numerical results for a Hirsch SVP (from ref. 2).

average horizontal ray velocity between turning points, the vertexing sound speed, and the action integral computed over one-half cycle.

In discussing the adiabatic invariant  $J = \oint (\sin \theta) dz/c$  (which is also called the action integral in analogy to classical mechanics, or the phase integral since it represents an area in phase space) we outlined a general scheme for efficiently computing an effective signal speed over long-range paths. Essentially, the procedure was reduced to a table-look-up method to obtain from a data base of previously computed  $\bar{c}$  vs  $J$  tables a particular  $\bar{c}$  value in each SVP region. A weighted average of these is then computed to obtain an average sound speed for the particular  $J$  value (that is, for the selected initial conditions for the ray trajectory) over the chosen path.

As a first step in implementing such an algorithm, we tested the hypothesis "J is conserved" for three range-dependent SVPs of the parabolic, Hirsch, and bilinear types using RAY1. The results tend to support the assumption that  $J$  is an invariant in range-dependent SVPs to an approximation suitable for practical signal speed calculations in typical ocean environments supporting RR rays.<sup>2</sup>

RAY2 provides a means for calculating the relationship between  $\bar{c}$  and  $J$  for arbitrary SVPs of the user's choice. Both RR and RSR rays are allowed and typical output can be presented as in figure 4. In addition to the  $\bar{c}$  vs  $J$  curves, one also needs a means for selecting an interval of  $J$  values characterizing the rays which carry most of the acoustic signal energy. This may be done by eliminating rays which exceed a cut-off depth or by including only those rays launched from the source (or arriving at the receiver) within a fixed angular window. RAY2 provides a list of ray turning point depths and a summary of the initial conditions to facilitate this selection.

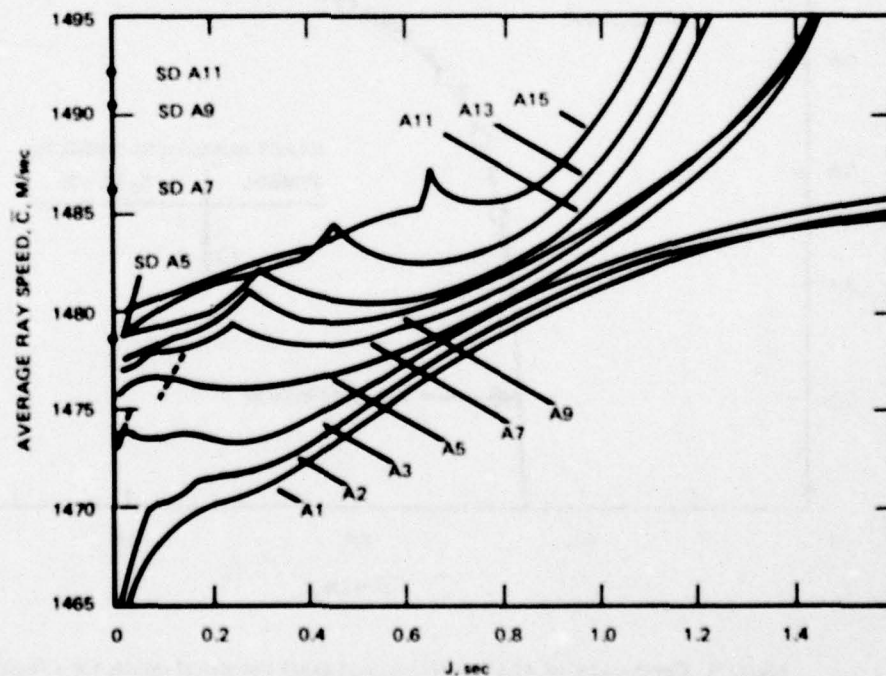


Figure 4. Relation between  $\bar{c}$  and  $J$  for a selection of SVPs (ref. 2).



Further discussion of RAY2, including input data requirements and internal logic, will be found in sections IV and V. It is worthwhile to stress here that RAY2 treats rays only in homogeneous (range independent) SVPs, and traces a family of 40 rays covering  $0.5^\circ$  to  $20^\circ$  in depression angle at the source out to the fifth vertexing point. (The latter parameters are simply adjusted by internal code changes.) Rays are traced over several half-cycles, even though a single half-cycle suffices to find  $\bar{c}$  and J, in order to check the accumulation of round-off errors in the integration routine. Since one is free to refine the mesh size, the trajectory may be made to reproduce itself on each loop to any accuracy (subject to machine constraints). One should use as large a step size as is compatible with the accuracy desired in order to minimize computations.

### III. INSTRUCTIONS FOR USING RAY1

Here we describe the required input data, output format, and general interpretation of results for RAY1.

#### A. INPUT REQUIREMENTS

Input data is read from cards under the Fortran free-field format. This format specification requires commas between separate data items but allows the items to be positioned arbitrarily on a data card. If a single read statement causes the input of data continued on to subsequent cards, no comma is required after the last item on each card. In this case, the card end itself serves as a legal delimiter between successive items.

On the first card, the integer variable ICASE must be punched. This should be the number of rays to be traced.

On the second card, and the remaining ICASE-1 cards, the data items as shown in table 2 must be punched. Typically one card is adequate to enter all items for a ray.

#### B. OUTPUT

RAY1 allows a quick check of the input data, by printing the variables for each case (each ray) considered in the form

```
CASE 1
DX = 1.2-02 METERS
XMAX = 1.180000+01 M
GRAD 1 = - 6.3510-02 (CHANNEL WIDTH GRADIENT)
GRAD 2 = 0.0000 Hz (AXIAL SPEED GRADIENT IN RANGE)
CO = 1.0000+00 M/SEC
AO = 1.0000+00 M
ZDOT = 3.6397 - 01 RADIANS or 2.0000+01 DEGREES
ZO = 0.0000 M
PROFILE: 1 (1=HIRSCH, 2=PARABOLIC, 3=BILINEAR)
```

If the mesh was refined during any cycle, the next line(s) will present this information in the form

```
MESH = 2 AT STEP 814
```

Table 2.

Card	Fortran Variable Name	Definition in RAY1
1	ICASE	Number of rays to be traced
2	DX	Range increment for Runge-Kutta raytracing routine (meters)
	XMAX	Cut-off range for raytracing (meters)
	GRAD1	Gradient in vertical scale length $a(x)$
	GRAD2	Gradient in axial sound speed $c_0(x)$ (Hz)
	CO	Initial axial sound speed (m/sec)
	AO	Initial vertical scale factor (meters)
	ZDOT	Initial ray slope ( $\tan\theta_0$ )
	ZO	Initial ray depth (meters)
	IPRINT	Control variable for printing a detailed path (0 : no ; 1 : yes)
	ITYPE	Control variable for SVP type (1 : Hirsch ; 2 : parabolic ; 3 : bilinear)
3	DX,...,ITYPE	Data for next ray

indicating one-half the input step size was used past step 814. These lines will not appear if no step size adjustment was made.

RAY1 employs a cut-off not only in range, but also in the number of steps calculated (presently 9999 steps are done) and in the channel width parameter. The user may inadvertently set up a constricting sound channel such that  $a(x)$  becomes zero and then negative in the allowed range. Raytracing is meaningless for such a profile. Rather than "bombing" under such conditions, RAY1 will test  $a(x)$ , find it is nonpositive, print a message of the form

CHANNEL WIDTH LESS THAN 0.01 AT STEP 704

terminate raytracing of the present ray, and go on to the next case, if there is one.

After RAY1 has completed tracing a given ray to XMAX (or for 9999 steps, or until  $a(x) \leq 0$ , whichever occurs first), it prints the summary, beginning with the number of axis crossings. (In contrast to RAY2 where the ocean surface is at  $z = 0$ , RAY1 always sets  $z = 0$  at the channel axis.) Then, for each axis crossing, the following data are printed:

STEP	RANGE	TIME	AVG(DX/DT)	A/AO	MAX Z	XP/AO	J
NO	(M)	(SEC)	(M/SEC)		(M)		(SEC)

Here AO denotes the initial value of the channel width parameter, and A/AO the dimensionless local value of  $a(x)$ . This is the same function  $a(x)$  appearing in eq (12) above. For constricting channels, the numbers in the A/AO column should be monotonically decreasing.

It is worthwhile noting that the  $AVG(DX/DT)$  column is derived from pairs of axis crossings and the first value corresponds to the average range rate or horizontal velocity between the initial ray position and the first turning point. For this reason, it may not represent an average between turning points. For the same reason, the last value is arbitrarily set to zero, there being no point beyond the last turning point with which to calculate  $\bar{c}$ . Similar comments apply to the entries in the J column, the (dimensionless) cycle period column  $XP/AO$ , and the maximum depth column.

#### IV. INSTRUCTIONS FOR USING RAY2

In this section we present information required to understand and run RAY2, beginning with a brief description of the necessary input parameters and the appropriate format for these, the output, and details of the program's scope and internal logical structure.

##### A. INPUT PARAMETER LIST

RAY2 consists of routines for tracing rays in user-provided SVPs. A cubic spline<sup>6</sup> is used to smooth the input data and to calculate interpolated values and derivatives of  $c(z)$  required by the Runge-Kutta routine. Output is provided in a summary form similar to that of RAY1. Detailed instructions for using RAY2 are provided in section IV, and section V contains a listing on the Fortran source code. All input data must be read from cards. Since freefield format is used for input (with one exception, an alphanumeric header card) one may simply place data items, in sequence, in any fields on the cards. Commas must appear between successive items, except when the next card is a continuation of the same read list items. This often occurs for the SVP data. In this case, the end of the card itself acts as a legal delimiter between the last item on the given card and the first item on the next card, and no comma is required.

RAY2 requires the input shown in table 3 immediately after the usual @XQT RAY2.ABS statement.

The variable NOSVPS tells RAY2 how many SVP functions are to follow. If this card is incorrectly punched (or misread), RAY2 will either end its computations before reaching the last data set or attempt to read beyond the last data set provided. If this card is missing, RAY2 will recognize NPTS as NOSVPS, and then fail (probably with a fatal execution error) when attempting to read card 3 under the format 2I10,2A6.

On card 2, NPTS is the number of pairs of depth (ZSVP) and sound speed (CSVP) values comprising the first SVP. If NPTS is mispunched RAY2 may attempt to read past the last card, or may stop before reading the last card, and proceed to recognize card  $j+1$  as SVP data or SVP data as card  $j+1$ . Results of such input errors could include many forms of abnormal termination.

Immediately following NPTS is IUNITS, which indicates the choice of units made by the user for SVP data. Set IUNITS equal to 1 if the units are to be meters and meters per second and 2 if feet and feet per second.

6. Mathpac, Univac Corp. (SPLN1 and SPLN2 are documented in a number of manuals covering resident subroutines.)



Table 3.

Card Number	Fortran Variable or Array Name	Input Format Spec (Variable Type)
1	NOSVPS	Free Field (Integer)
2	NPTS, IUNITS, MSG(1) MSG(2)	2I10,2A6
3	ZSVP(1), CSVP(1) ... ZSVP(i), CSVP(i)	Free Field (Real)
4	ZSVP(i+1), CSVP(i+1), ...	Free Field (Real)
j	... ZSVP(NPTS), CSVP(NPTS)	Free Field (Real)
j+1	DX, ZO, ZMAX, IPLOT	Free Field (Real, Real, Real, Integer)
j+2, : k	data for next SVP, beginning with NPTS, IUNITS, MSG(1), MSG(2), and ending with DX, ZO, etc.	
k+1, etc.	data for last of NOSVPS data sets	

MSG(1) and MSG(2) provide a title for the SVP to follow, consisting of 12 characters selected from the full range of UNIVAC 1110 Fortran and entered in columns 21-32 of card 2.

Note that card 2 is read under a formatted input specification.

Beginning with card 3, and continuing on subsequent cards if necessary, is the first set of SVP data. As many pairs may be entered on one card as space permits and pairs of (ZSVP, CSVP) values may be split, with ZSVP(i) ending one card and CSVP(i) beginning the next card.

Four variables which control raytracing are entered on the card after the last SVP data card. DX, ZO, and ZMAX are the range increment for the Runge-Kutta algorithm, the initial ray depth, and the maximum depth allowed for a ray, respectively. *These variables are interpreted by RAY2 as being expressed in meters.* IPLOT should be set to 0 if one desires printed output, and 1 if plots are desired in addition. Typical values for DX should be approximately one-sixteenth of a ray cycle period, for coarse results, and less for more accurate raytracing. If a ray exceeds depth ZMAX, the remaining (steeper) rays are not traced and RAY2 attempts to read the next SVP data set.

## B. OUTPUT

RAY2 is designed to allow the user an immediate check of all input. The first line printed after the @XQT statement should agree with the input variable NOSVPS, and reads:

\*\*\* THIS RUN CONSISTS OF (NOSVPS) SVP(S) \*\*\*

The second output line consists of the 12 character message string MSG(1), MSG(2) imbedded as follows:

\*\*\* SVP : (MSG(1), MSG(2)) \*\*\*

This simply identifies the particular SVP being computed. If several SVPs are to be run, one such header message appears at the start of the output for each SVP.

The header message is followed immediately by a line that checks the choice of units for the SVP data, and reads:

USER INPUT UNITS FOR THE SVP : (1 or 2) (1 : M, M/SEC ; 2 : FT, FT/SEC)

IUNITS and the units choice (1 or 2) should agree. Next the SVP is printed as a pair of columns labeled DEPTH and c. There should be NPTS pairs of values.

After the SVP data, RAY2 prints the control parameters specifying how rays are to be traced, namely DX, ZO, and ZMAX.

Beginning with the line

CASE NUMBER : 1 .

RAY2 prints, as presently structured, 40 ray-path summaries, for the rays which are launched from depth ZO at the angles  $-0.5^\circ$ ,  $-1.0^\circ$ ,  $-1.5^\circ$ , ...,  $-20^\circ$ , with respect to horizontal. Each case is summarized by a set of initial conditions printed in the form

CASE NUMBER : 1  
INITIAL ANGLE = 0.5 DEGREES  
INITIAL SOUND SPEED = 1495.6 M/SEC  
PREDICTED VERTEXING SPEED = 1500.2 M/SEC

The first and second lines are redundant since the initial angle associated with a given case is always one-half the case number. Nevertheless, it is useful to see at a glance the angle of the ray being considered, and if internal changes are made to produce a different angular interval for rays, these two lines would serve as checks on the code changes and would simplify some data analysis.

The initial sound speed is computed by the spline curve fitting routine SPLN1,<sup>6</sup> and used to compute a predicted vertex speed according to Snell's law,

$$c_{\text{vertex}} = c(z_0) / \cos \theta(z_0) .$$

Each case is also summarized by a table showing the history of ray turning points. As presently written RAY2 automatically traces rays through four turning points. The variables printed at each turning point (with the exception of J for the first turning point and the average speed for the last turning point) are:

K, XTP, TTP, ZTP, CTP, J(K), AVGSP .



These stand for the turning point number,  $K$ , the range to the  $K$ th turning point, the time elapsed at the  $K$ th turning point, the depth of the  $K$ th turning point, the ray speed at the  $K$ th turning point, the action integral  $\int \sin\theta \, dz/c$  computed over the last one-half cycle, and the average horizontal ray speed from the  $K$ th to the  $(K+1)$ st turning point.

Figure 5 illustrates the physical significance of these summary data items. Note that the first value printed in the  $J$  column is really an incomplete integral, evaluated from the starting depth  $z_0$  to the first turning point, and should be ignored. RAY2 computes the average horizontal ray velocity between pairs of turning points. The first AVGSP value printed out is associated with the first and second turning points, and the fourth value is automatically set to zero.

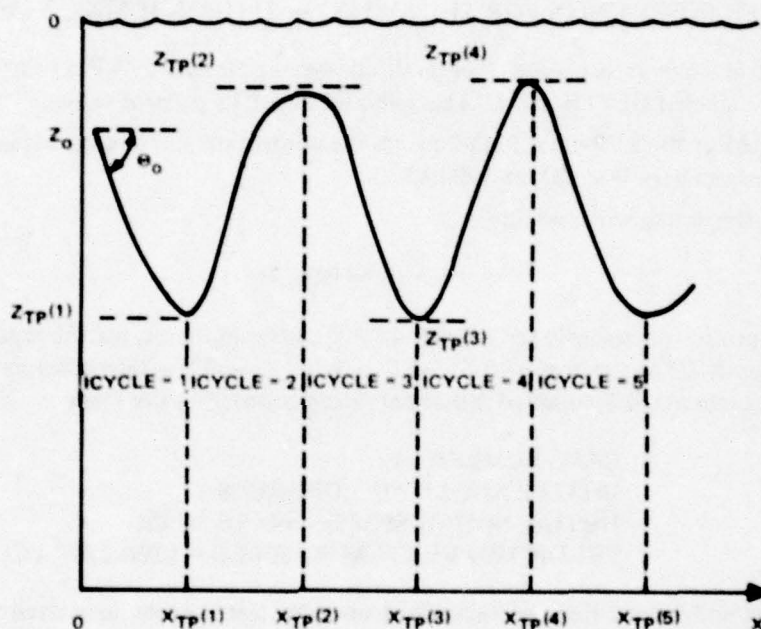


Figure 5. A sketch of the physical meaning of the summary data items in RAY2.

## V. INTERNAL LOGICAL STRUCTURE OF RAY1 AND RAY2

In this section we shall describe the logical structure of the Fortran routines comprising RAY1 and RAY2. Special emphasis is placed on the areas in which slight modifications in these codes would enhance their usefulness, particularly in the direction of permitting better output (e.g., plots) and more flexibility through user-selected input variables, beyond those now available.

### A. INTERNAL STRUCTURE OF RAY1

As it is presently written, RAY1 contains comment cards defining most of the variables of interest (see section VI). A flowchart of RAY1 appears in figure 6. ICASE is

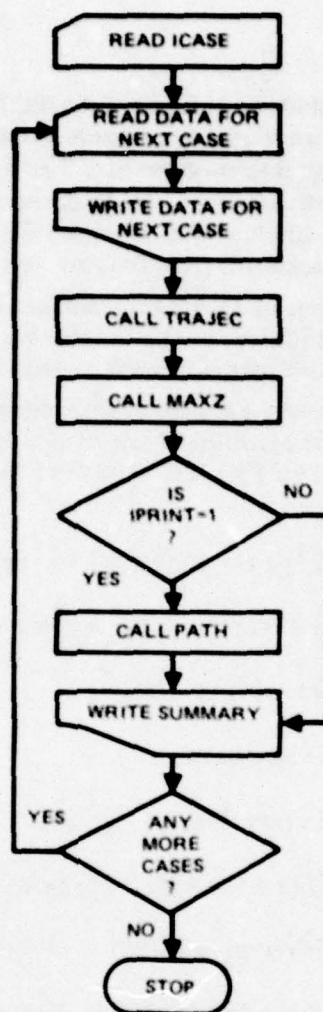


Figure 6. Flowchart of RAY1.

the number of cases to be considered. Each case consists of a particular choice for an SVP, initial ray depth and slope, and parameters for the range step, maximum range, and gradients of the range-dependent parameters (axial sound speed and channel width parameter in eq (12)). In addition, RAY1 reads IPRINT which allows or suppresses a longer printout of the trajectory.

An extremely valuable addition to RAY1 would be a plotting routine which simply plots the ray paths. One could then observe immediately (without calling the subroutine PATH) the effect of squeezing or expanding SVPs on ray paths. A second much needed improvement consists of permitting several rays to be traced in a given range-dependent SVP, without the requirement of punching all SVP data and other parameters anew for each ray.

The subroutine TRAJEC computes a ray path, including the time and average horizontal velocity at each turning point, and the action integral over each half-cycle. Beginning at line 26 (see section VI) TRAJEC computes the new ray slope (DERIZ). These instructions end at line 40 of TRAJEC, and consist of the Runge-Kutta algorithm mentioned earlier.

Once an advanced value of  $z$  is found, TRAJEC finds the new sound speed at this depth and range, which in turn is used to compute a time increment given by  $\Delta t = \Delta s/c$ , and a new increment of the action integral given by  $c^{-1} \sin \theta \Delta z$ . These steps correspond to lines 42 through 55. Two tests are made here to insure that the user has not allowed the channel width parameter to vanish, and to avoid any illegal (or rather invalid) reference to array elements by looking backwards from the very first step of the raytracing.

The remaining portions of TRAJEC handle axis crossings and adjust the step size should there be fewer than 150 steps per half-cycle. We recommend that an input variable be added to permit varying this particular choice at run time.

In section II we derived the Euler-Lagrange equation, eq (7), for Fermat's variational principle. RAY1 calculates the right-hand side of this equation of motion in the function subroutine F, which is called by TRAJEC. The three SVPs in equations (12) lead, respectively, to the results

$$F = -2(1 + \dot{z}^2) z/(a^2 + z^2) + \dot{z}(1 + \dot{z}^2) g_2/c_0 - 2 \dot{z}(1 + \dot{z}^2) (z^2/a) g_1/(a^2 + z^2) , \quad (13a)$$

$$F = -(z/a)^2 (1 + \dot{z}^2)/(1 - (z/a)^2) + \dot{z}(1 + \dot{z}^2) g_2/c_0 - \dot{z}(1 + \dot{z}^2) (z^2/a^3) g_1/(1 - z^2/a^2) , \quad (13b)$$

$$F = \pm(1 + \dot{z}^2)/(a + |z|) + \dot{z}(1 + \dot{z}^2) g_2/c_0 - \dot{z}(1 + \dot{z}^2) |z| g_1/a(a + |z|) , \quad z \leq 0 (> 0) , \quad (13c)$$

as one can verify easily by direct differentiation. Here  $g_1$  and  $g_2$  are respectively  $da/dx$  and  $dc(z=0)/dx$ .

MAXZ and PATH are short routines. The former searches each half cycle of the trajectory and returns a list of the maximum off-axis distance reached by the ray. The latter prints 250 points equally spaced along the trajectory, or as many points as are found before the maximum range is reached.

RAY1 should be expanded to handle a wider class of range-dependent analytic SVPs, and to permit connecting range-independent SVPs smoothly, as discussed in section II.

## B. INTERNAL STRUCTURE OF RAY2

RAY2 consists of only two routines and two cubic spline routines resident on the NOSC UNIVAC 1110.<sup>6</sup> Unlike RAY1, RAY2 does provide a plot subroutine and uses any user-provided SVP. We recommend that the plot routine calls be modified to allow several rays to be plotted on a single graph. Also desirable would be a plot of the user-input SVP as smoothed by the spline routines.

A flowchart of RAY2 is given in figure 7. Although somewhat complicated in appearance, the flowchart involves only three basic loops. The outermost, which corresponds



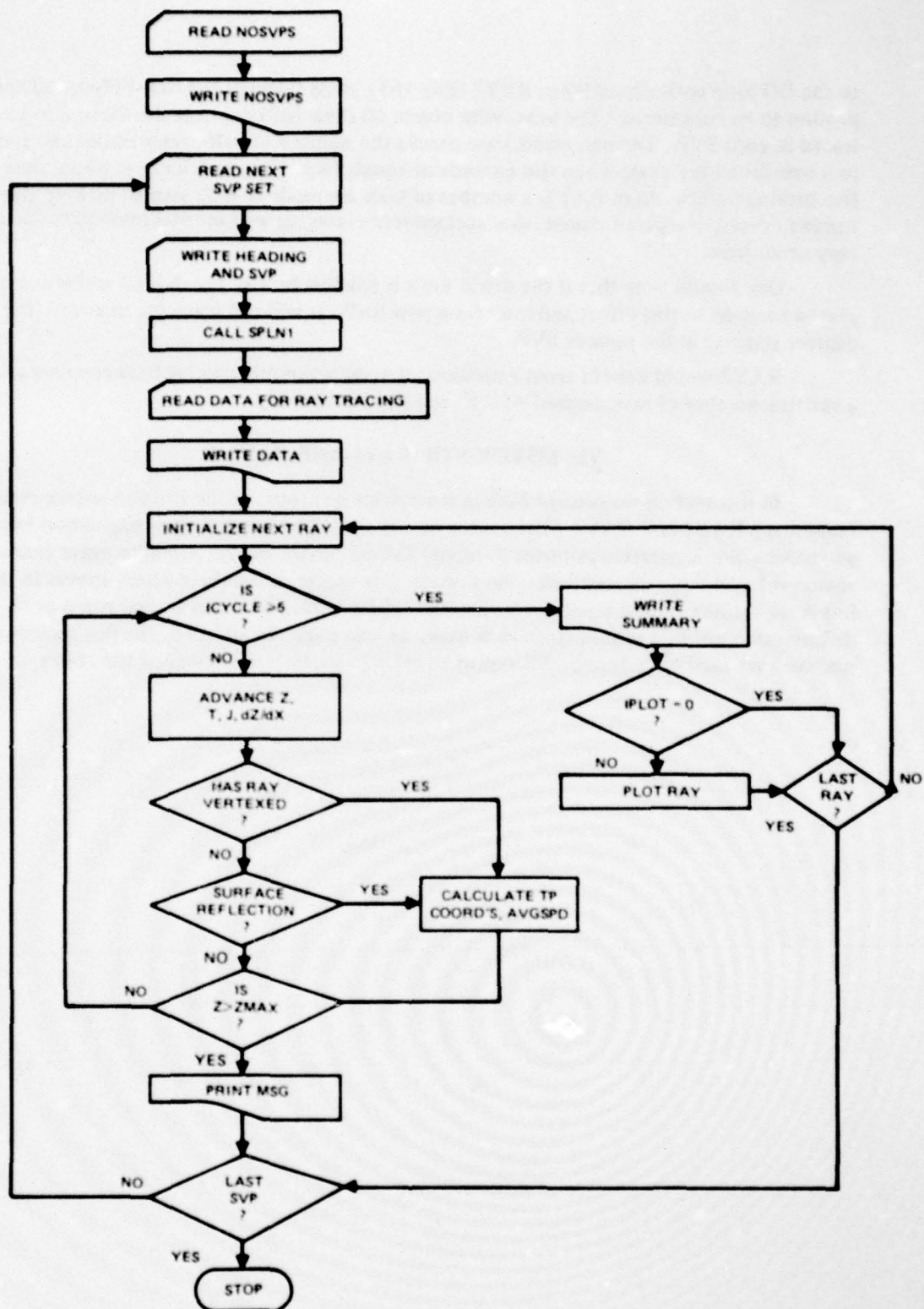


Figure 7. Flowchart of RAY2.

to the DO loop with object 90 in RAY2 (line 163), steps through the NOSVPS sound speed profiles to be considered. The next, with object 60 (line 162) controls the 40 rays to be traced in each SVP. The innermost loop checks the number of half-cycles traced and jumps to a new initial ray angle when this exceeds or equals five. Hence each ray is traced over five turning points. As in RAY1, a number of tests are made at each step to pick up the turning points, except, of course, that surface reflections, as well as total internal reflections, may occur here.

One should note that if the depth limit is reached by any ray, RAY2 will automatically print a message to this effect and look for a new SVP. It will not trace the next ray (0.5 degrees steeper) in the present SVP.

RAY2 would benefit from a revision allowing a variable spacing between rays and a variable number of rays, instead of 0.5° and 40, respectively.

## VI. LISTINGS OF RAY1 AND RAY2

In this section we present listings (computer printout) of the Fortran source code comprising RAY1 and RAY2. The reader should note that in some cases pagination becomes awkward when converting printout to report format. In particular, separate pages cannot always refer to separate routines. The Fortran line sequence numbers which appear in the left-hand column should therefore be used to follow a routine across several pages or to distinguish multiple routines from each other on one page. In addition, the line sequence numbers are used elsewhere in this report to refer to particular sections of the codes.

















```

SUBROUTINE WAZ2
C THIS ROUTINE USES THE POINTERS IN ARRAY J TO FIND THE MAXIMUM
C NO. OCCURRENCE OVER EACH CYCLE
COMMON/RESULT/RESULT(1000),X(1000),DEZ(1000),ICOUNT,
C J(200,4),X(200),ACT(200),Y(200),A(200),N
ICOUNT=0
DO 10 I=1,ICNTM1
  X(I)=1
  J(I,1)=1
  J(I,2)=1
  J(I,3)=1
  J(I,4)=1
  X(I)=1
  DEZ(I)=1
  DO 20 K=1,4
    IF (ABS(J(I,K)-ACT(I)))=0
      ICOUNT=ICOUNT+1
  20 CONTINUE
  RETURN
END

```



CASE 1  
 D= 1.0000-02 METERS  
 S= 1.10000-01 \*  
 GA= 10-6.3510-02 CHANNEL WIDTH GRADIENT  
 GA= 20 0.0000 WZ LATERAL SPEED GRADIENT IN RANGES  
 CO= 1.0000-00 W/SFC  
 AO= 1.0000-00 W  
 ZO= 3.6307-01 RADIANS OR 2.0000-01 DEGREES  
 ZO= 0.0000 W  
 PROFILE: 1 110109CM, Z00000POLIC, 3001LINFM)

# RESULTS:

WFSMO 2 AT STEP 150

WFSMO 3 AT STEP 1520

MAXIMUM DISTANCE AT STEP 1562

CHANNEL WIDTH LESS THAN 0.01 AT STEP 1562

AXIS CROSSINGS: 8

SUMMARY OF AXIS CROSSINGS:

NUMBER	STEP	RANGE	NO.	TIME	AVG (M/SEC)	A/40	MAX Z	W/40	J
				SEC					
1	1	0.00000	0.00000	0.00000	9.774316-01	1.000000-00	3.266505-01	2.676209-00	1.000000-01
2	249	2.676209-00	2.676209-00	2.676209-00	9.774316-01	9.300390-01	-2.077873-01	2.190655-00	1.000000-01
3	98	4.866666-00	4.866666-00	4.866666-00	9.774316-01	4.909565-01	2.718099-01	1.792687-00	1.000000-01
4	447	8.859531-00	8.859531-00	8.859531-00	9.774316-01	5.770519-01	-2.077873-01	1.466395-00	1.000000-01
5	814	8.125996-00	8.125996-00	8.125996-00	9.774316-01	4.819212-01	2.718099-01	1.194519-00	1.000000-01
6	1053	9.320000-00	9.320000-00	9.320000-00	9.774316-01	4.080573-01	-2.077873-01	9.786380-01	1.000000-01
7	1299	1.030010-01	1.030010-01	1.030010-01	9.774316-01	3.658805-01	1.923680-01	7.989249-01	1.000000-01
8	1408	1.109003-01	1.109003-01	1.109003-01	9.774316-01	2.651004-01	-1.789361-01	6.501577-01	1.000000-01
9	1536	1.174010-01	1.174010-01	1.174010-01	9.774316-01	2.538081-01	0.000000	0.000000	0.000000

CASE 2  
 D= 1.0000-02 METERS  
 WAKE 2.341700-01 "  
 GRAD1=3.1757-02 CHANNEL WIDTH GRADIENT  
 GRAD2= 0.0000 W/ LATERAL SPEED GRADIENT IN RANGEL  
 CO= 1.0000-00 W/SEC  
 AC= 1.0000-00 "  
 ZONE 3.6397-01 RADIANS OR 2.0000-01 DEGREES  
 ZONE 0.0000 "  
 PROFILE: 1 11-HINSCHE, 20-ANNUAL, 300-LINER

# RESULTS:

WESNO 2 AT STEP 1627

WESNO 3 AT STEP 2952

MAXIMUM DISTANCE AT STEP 3295

CHANNEL WIDTH LESS THAN 0.01 AT STEP 3295

AXIS CROSSINGS: 16

SUMMARY OF AXIS CROSSINGS:

NUMBER	STEP	NO.	RANGE (M)	TIME (SEC)	AVG(DR/DT) (M/SEC)	A/AO	MAX Z (M)	SP/AD	J (SEC)
1	1	1	0.00000	0.00000	9.078637-01	1.000000-00	3.341714-01	2.809510-00	3.683913-01
2	282	2	2.809510-00	2.815525-00	9.073717-01	9.107284-01	-3.189649-01	2.542109-00	3.689492-01
3	637	3	5.351610-00	5.364276-00	9.068184-01	9.300407-01	3.055518-01	2.300038-00	3.673702-01
4	747	4	7.451637-00	7.471653-00	9.061204-01	7.570043-01	-2.008947-01	2.000086-00	3.687151-01
5	976	5	9.732592-00	9.760643-00	9.052644-01	9.902337-01	2.779648-01	1.882468-00	3.678670-01
6	1193	6	1.161501-01	1.145207-01	9.042218-01	9.311421-01	-2.457244-01	1.702908-00	3.677424-01
7	1333	7	1.331782-01	1.336477-01	9.029444-01	5.776440-01	2.541484-01	1.540115-00	3.662537-01
8	1487	8	1.485793-01	1.491503-01	9.013942-01	5.781566-01	-2.431974-01	1.392769-00	3.698338-01
9	1627	9	1.625070-01	1.632064-01	9.006336-01	5.830244-01	2.379394-01	1.254686-00	2.190299-01
10	1877	10	1.750639-01	1.758979-01	9.071947-01	5.440819-01	-2.231793-01	1.138731-00	1.827184-01
11	2104	11	1.844412-01	1.874329-01	9.041914-01	5.079147-01	2.139648-01	1.029122-00	1.841937-01
12	2310	12	1.947324-01	1.978873-01	9.009743-01	3.742349-01	-2.052928-01	9.297481-01	1.839958-01
13	2494	13	2.040301-01	2.073653-01	9.068222-01	3.467102-01	1.971329-01	8.396776-01	1.806624-01
14	2644	14	2.144269-01	2.159613-01	9.071774-01	3.194446-01	-1.894620-01	7.579539-01	1.899812-01
15	2814	15	2.220044-01	2.237610-01	9.045452-01	2.949742-01	1.872616-01	6.837816-01	1.819174-01
16	2952	16	2.288492-01	2.308420-01	9.047204-01	2.733594-01	-1.755452-01	6.140747-01	1.844466-01
17	3194	17	2.349450-01	2.372604-01	0.000000	2.537542-01	0.000000	0.000000	0.000000

CASE 3  
 DOW 1.0000-02 METERS  
 SHAPE 3.542500-01 M  
 GRADE 2.1171-02 (CHANNEL WIDTH GRADIENT)  
 GRADE 0.0000 M (LATERAL SPEED GRADIENT IN MANGS)  
 COE 1.0000-00 M/SEC  
 AOE 1.0000-00 M  
 ZONE 3.6367-01 RADIAN ON 1.9985-01 DEGREES  
 ZOE 0.0000 M  
 PROFILE 1 (HELMHOLTZ, PARABOLIC, LINEAR)

# RESULTS:

WESHO 2 AT STEP 2302

WESHO 3 AT STEP 4362

MAXIMUM DISTANCE AT STEP 5204

CHANNEL WIDTH LESS THAN 0.01 AT STEP 5204

AXIS CROSSINGS: 24

SUMMARY OF AXIS CROSSINGS:

NUMBER	STEP	NO.	TIME (SEC)	AVG. (M/SEC)	A/SO	MAX Z (M)	BP/RO	J (SEC)
1	1	0.000000	0.000000	9.974918-01	1.000000-00	3.345038-01	2.856254-00	5.523896-01
2	247	7.866276-00	2.862144-00	9.974502-01	9.985303-01	-2.261922-01	2.872080-00	5.521909-01
3	554	5.523896-00	5.523896-00	9.971145-01	9.929011-01	3.162336-01	2.899693-00	5.509326-01
4	804	8.028004-00	8.028004-00	9.969374-01	8.900391-01	-3.046439-01	2.338308-00	5.529961-01
5	1038	1.036638-01	1.036249-01	9.968071-01	7.806331-01	2.973811-01	2.187939-00	5.518508-01
6	1264	1.265383-01	1.258760-01	9.960055-01	7.872229-01	-2.886993-01	2.046160-00	5.520455-01
7	1462	1.465999-01	1.464194-01	9.958392-01	6.906037-01	2.798350-01	1.913962-00	5.499095-01
8	1653	1.651393-01	1.654667-01	9.947958-01	6.003836-01	-2.715329-01	1.790195-00	5.533706-01
9	1832	1.830612-01	1.834673-01	9.926542-01	6.124833-01	2.632290-01	1.679370-00	5.016187-01
10	1999	1.997899-01	2.004862-01	9.912111-01	5.270353-01	-2.558178-01	1.565957-00	3.672142-01
11	2164	2.165445-01	2.162526-01	9.922468-01	5.538828-01	2.483761-01	1.446973-00	3.666186-01
12	2302	2.300693-01	2.310120-01	9.903818-01	5.126781-01	-2.412822-01	1.346723-00	3.676180-01
13	2476	2.473365-01	2.477917-01	9.879803-01	4.939855-01	2.349933-01	1.280748-00	3.673859-01
14	2631	2.656481-01	2.657730-01	9.884490-01	4.568709-01	-2.277665-01	1.197481-00	3.693153-01
15	3071	2.685190-01	2.688951-01	9.880161-01	4.215185-01	2.213871-01	1.119499-00	3.654799-01
16	3294	2.797139-01	2.811894-01	9.893585-01	4.078177-01	-2.152551-01	1.046961-00	3.675425-01
17	3504	2.901786-01	2.918141-01	9.824222-01	3.954631-01	2.093580-01	9.780591-00	3.676690-01
18	3700	2.999591-01	3.017855-01	9.804122-01	3.849566-01	-2.034980-01	9.139840-01	1.894097-01
19	3843	3.090990-01	3.110880-01	9.774400-01	3.754046-01	1.982544-01	8.539577-01	1.819044-01
20	4053	3.176385-01	3.198227-01	9.745105-01	3.275275-01	-1.930188-01	7.876823-01	1.864395-01
21	4213	3.256154-01	3.280081-01	9.709255-01	3.104397-01	1.880383-01	7.499570-01	1.836303-01
22	4342	3.330648-01	3.356808-01	9.656879-01	2.904883-01	-1.832751-01	6.931014-01	1.832889-01
23	4636	3.399955-01	3.428888-01	9.621902-01	2.801866-01	1.786803-01	6.492610-01	1.828662-01
24	4894	3.466886-01	3.496046-01	9.563369-01	2.644991-01	-1.742833-01	6.057988-01	1.845954-01
25	5141	3.525465-01	3.559371-01	9.000000	2.534238-01	0.000000	0.000000	0.000000



CASE N  
 DIA 1.0000-02 METERS  
 WAVE 0.723000-01 M  
 GRADE 1.5400-02 CHANNEL WIDTH GRADIENT  
 GRADE 0.0000 MZ LATERAL SPEED GRADIENT IN RANGES  
 CO 1.0000-00 M/SEC  
 AO 1.0000-00 M  
 ZONE 3.0000-01 RADIANS OR 2.0000-01 DEGREES  
 ZON 0.0000 M  
 PROFILE 1 LINEAR, 2 PARABOLIC, 3 BILINEAR

# RESULTS:

WAVE 2 AT STEP 2973

WAVE 3 AT STEP 5910

MAXIMUM DISTANCE AT STEP 703

CHANNEL WIDTH LESS THAN 0.01 AT STEP 703

AXIS CROSSINGS: 32

## SUMMARY OF AXIS CROSSINGS:

NUMBER	STEP	WAVE	NO.	TIME (SEC)	AVG WAVE (M/SEC)	A/D	MAX Z (M)	EP/40	J (SEC)
1	1	0.000000	1	0.000000	0.000000	1.000000	3.300530-01	2.079400-00	7.361992-01
2	240	2.079400-00	2	2.079400	0.000000	0.000000	-3.300530-01	2.079400-00	7.361992-01
3	543	0.000000	3	0.000000	0.000000	0.000000	3.300530-01	2.079400-00	7.361992-01
4	874	0.000000	4	0.000000	0.000000	0.000000	-3.300530-01	2.079400-00	7.361992-01
5	1072	1.070274-01	5	1.070274	1.070274	1.070274	3.300530-01	2.079400-00	7.361992-01
6	1308	1.308023-01	6	1.308023	1.308023	1.308023	-3.300530-01	2.079400-00	7.361992-01
7	1632	1.632026-01	7	1.632026	1.632026	1.632026	3.300530-01	2.079400-00	7.361992-01
8	1745	1.745035-01	8	1.745035	1.745035	1.745035	-3.300530-01	2.079400-00	7.361992-01
9	1948	1.948042-01	9	1.948042	1.948042	1.948042	3.300530-01	2.079400-00	7.361992-01
10	2141	2.141057-01	10	2.141057	2.141057	2.141057	-3.300530-01	2.079400-00	7.361992-01
11	2324	2.322079-01	11	2.322079	2.322079	2.322079	3.300530-01	2.079400-00	7.361992-01
12	2499	2.499091-01	12	2.499091	2.499091	2.499091	-3.300530-01	2.079400-00	7.361992-01
13	2665	2.663093-01	13	2.663093	2.663093	2.663093	3.300530-01	2.079400-00	7.361992-01
14	2823	2.821315-01	14	2.821315	2.821315	2.821315	-3.300530-01	2.079400-00	7.361992-01
15	2973	2.971451-01	15	2.971451	2.971451	2.971451	3.300530-01	2.079400-00	7.361992-01
16	3267	3.113743-01	16	3.113743	3.113743	3.113743	-3.300530-01	2.079400-00	7.361992-01
17	3629	3.749576-01	17	3.749576	3.749576	3.749576	3.300530-01	2.079400-00	7.361992-01
18	3782	3.378634-01	18	3.378634	3.378634	3.378634	-3.300530-01	2.079400-00	7.361992-01
19	4032	3.501396-01	19	3.501396	3.501396	3.501396	3.300530-01	2.079400-00	7.361992-01
20	4264	3.618113-01	20	3.618113	3.618113	3.618113	-3.300530-01	2.079400-00	7.361992-01
21	4489	3.729091-01	21	3.729091	3.729091	3.729091	3.300530-01	2.079400-00	7.361992-01
22	4696	3.834572-01	22	3.834572	3.834572	3.834572	-3.300530-01	2.079400-00	7.361992-01
23	4899	3.934815-01	23	3.934815	3.934815	3.934815	3.300530-01	2.079400-00	7.361992-01
24	5090	4.030147-01	24	4.030147	4.030147	4.030147	-3.300530-01	2.079400-00	7.361992-01
25	5271	4.120753-01	25	4.120753	4.120753	4.120753	3.300530-01	2.079400-00	7.361992-01
26	5453	4.206447-01	26	4.206447	4.206447	4.206447	-3.300530-01	2.079400-00	7.361992-01
27	5607	4.288450-01	27	4.288450	4.288450	4.288450	3.300530-01	2.079400-00	7.361992-01
28	5762	4.366371-01	28	4.366371	4.366371	4.366371	-3.300530-01	2.079400-00	7.361992-01
29	5910	4.440203-01	29	4.440203	4.440203	4.440203	3.300530-01	2.079400-00	7.361992-01
30	6189	4.510082-01	30	4.510082	4.510082	4.510082	-3.300530-01	2.079400-00	7.361992-01
31	6456	4.576681-01	31	4.576681	4.576681	4.576681	3.300530-01	2.079400-00	7.361992-01
32	6709	4.639916-01	32	4.639916	4.639916	4.639916	-3.300530-01	2.079400-00	7.361992-01
33	6949	4.699997-01	33	4.699997	4.699997	4.699997	3.300530-01	2.079400-00	7.361992-01

THIS PAGE IS BEST QUALITY FRAGMENT  
 FROM COPY FURNISHED TO DOD

[illegible]

```

000043 23. READ(5,1002) (ZSUP(I),ZSUP(I),I=1,IMPTS)
000044 24. WRITE(6,1043) (ZSUP(I),I=1,IMPTS)
000045 25. 104 FORMAT(10I8,"---SUP: ",2A6," ---")
000046 26. " - USED INPUT UNITS FOR THE SUP: "
000047 27. " 13. - (1/M, M/SEC, 2: 17, 17/SEC) "
000048 28. IF (IUNIT15.EQ.1) WRITE(6,107)
000049 29. IF (IUNIT16.EQ.2) WRITE(6,108)
000050 30. 107 FORMAT(10I8," DEPTH(M)",4A6," (M/SEC) ")
000051 31. 108 FORMAT(10I8," DEPTH(M)",4A6," (M/SEC) ")
000052 32. DO 1 I=1,IMPTS
000053 33. 1 WRITE(6,100) (ZSUP(I),ZSUP(I))
000054 34. " ---SKIP THE PLOTTING FOR NOW---"
000055 35. IF (IUNIT15.EQ.100160 TO 5)
000056 36. IF (IUNIT16.EQ.1)
000057 37. "CALL BLABEL," SOUND SPEED (M/SEC) ",100)
000058 38. IF (IUNIT15.EQ.2)
000059 39. "CALL BLABEL," SOUND SPEED (M/SEC) ",100)
000060 40. IF (IUNIT16.EQ.1)
000061 41. "CALL BLABEL," DEPTH (M) ",100)
000062 42. IF (IUNIT15.EQ.2)
000063 43. "CALL BLABEL," DEPTH (M) ",100)
000064 44. CALL LIMPT(CSUP,ZSUP,50)
000065 45. 5 CONTINUE
000066 46. C
000067 47. C ---CONVERT TO METRIC UNITS FOR REPAIRING OF CALCULATIONS ---
000068 48. IF (IUNIT15.EQ.1)60 TO 10
000069 49. DO 8 I=1,IMPTS
000070 50. ZSUP(I)=ZSUP(I)*0.3048004
000071 51. 8 CSUP(I)=ZSUP(I)*0.3048004
000072 52. 10 CONTINUE
000073 53. C ---FIT A SINE CURVE TO THE INPUT SUP---
000074 54. S11)=0.
000075 55. S12)=0.
000076 56. CALL SPLIN(IMPTS,ZSUP,CSUP,2,0,(COEF,5))
000077 57. C --- GET INPUT DATA AND BEGIN THE RAY ANGLE LOOP ---
000078 58. READ(5,1003) (S,20,ZMAY,IPLCT
000079 59. WRITE(6,1003) (S,20,ZMAY
000080 60. 104 /COMPT(100," INPUT PARAMETERS: ",10I8," 1PEB,2," METERS"/
000081 61. " - INITIAL DEPTH=",1PEB,2," METERS"/
000082 62. " - MAX ALLOWED DEPTH=",1PEB,2," METERS"/)
000083 63. DO 40 I=1,1,40
000084 64. RAYANG=FLOAT(I*RAY)/2.
000085 65. 11=RAY
000086 66. V1)=20
000087 67. CALL SPLIN2(IMPTS,ZSUP,CSUP,COEF,V)
000088 68. COEFF1423)/COS(0.01745329*RAYANG)
000089 69. WRITE(6,1011) (RAYANG,V123),CCRIT
000090 70. 101 FORMAT(10I8," CASE NUMBER: ",14/
000091 71. " - INITIAL ANGLE=",1PEB,2," DEGREES"/
000092 72. " - INITIAL SOUND SPEED=",4PE10,1," M/SEC"/
000093 73. " - PREDICTED VELOCITY SPEED=",4PE10,1," M/SEC")
000094 74. C
000095 75. C --- CALCULATE RAY PATH, AVG. SPEED, AND ACTION ---
000096 76. Z11)=20
000097 77. X11)=0.
000098 78. DEBIT(11)=TAN(C.01745329*RAYANG)
000099 79. 10255
000100 80. 10256
000101 81. 10257
000102 82. 10258
000103 83. 10259
000104 84. 10260
000105 85. 10261
000106 86. 10262
000107 87. 10263
000108 88. 10264
000109 89. 10265
000110 90. 10266
000111 91. 10267
000112 92. 10268
000113 93. 10269
000114 94. 10270
000115 95. 10271
000116 96. 10272
000117 97. 10273
000118 98. 10274
000119 99. 10275
000120 100. 10276
000121 101. 10277
000122 102. 10278
000123 103. 10279
000124 104. 10280
000125 105. 10281
000126 106. 10282
000127 107. 10283
000128 108. 10284
000129 109. 10285
000130 110. 10286
000131 111. 10287
000132 112. 10288
000133 113. 10289
000134 114. 10290
000135 115. 10291
000136 116. 10292
000137 117. 10293
000138 118. 10294
000139 119. 10295
000140 120. 10296
000141 121. 10297
000142 122. 10298
000143 123. 10299
000144 124. 10300
000145 125. 10301
000146 126. 10302
000147 127. 10303
000148 128. 10304
000149 129. 10305
000150 130. 10306
000151 131. 10307
000152 132. 10308
000153 133. 10309
000154 134. 10310
000155 135. 10311
000156 136. 10312
000157 137. 10313
000158 138. 10314
000159 139. 10315
000160 140. 10316
000161 141. 10317
000162 142. 10318
000163 143. 10319
000164 144. 10320
000165 145. 10321
000166 146. 10322
000167 147. 10323
000168 148. 10324
000169 149. 10325
000170 150. 10326
000171 151. 10327
000172 152. 10328
000173 153. 10329
000174 154. 10330
000175 155. 10331
000176 156. 10332
000177 157. 10333
000178 158. 10334
000179 159. 10335
000180 160. 10336
000181 161. 10337
000182 162. 10338
000183 163. 10339
000184 164. 10340
000185 165. 10341
000186 166. 10342
000187 167. 10343
000188 168. 10344
000189 169. 10345
000190 170. 10346
000191 171. 10347
000192 172. 10348
000193 173. 10349
000194 174. 10350
000195 175. 10351
000196 176. 10352
000197 177. 10353
000198 178. 10354
000199 179. 10355
000200 180. 10356
000201 181. 10357
000202 182. 10358
000203 183. 10359
000204 184. 10360
000205 185. 10361
000206 186. 10362
000207 187. 10363
000208 188. 10364
000209 189. 10365
000210 190. 10366
000211 191. 10367
000212 192. 10368
000213 193. 10369
000214 194. 10370
000215 195. 10371
000216 196. 10372
000217 197. 10373
000218 198. 10374
000219 199. 10375
000220 200. 10376
000221 201. 10377
000222 202. 10378
000223 203. 10379
000224 204. 10380
000225 205. 10381
000226 206. 10382
000227 207. 10383
000228 208. 10384
000229 209. 10385
000230 210. 10386
000231 211. 10387
000232 212. 10388
000233 213. 10389
000234 214. 10390
000235 215. 10391
000236 216. 10392
000237 217. 10393
000238 218. 10394
000239 219. 10395
000240 220. 10396
000241 221. 10397
000242 222. 10398
000243 223. 10399
000244 224. 10400
000245 225. 10401
000246 226. 1040
```







10	CG109
20	CG161
30	CG161
40	CG161
50	CG161
60	CG161
70	CG161
80	CG161
90	CG161
100	CG161
110	CG161
120	CG161

THIS PAGE IS BEST QUALITY PRINT



800-2400 1000

...TMS TWO (205111) 00 1 104(5)000

```

...TYP: MACH A15 ...
...IMPORT UNITS FOR THE TYP: 2 (1:0.0/100;2:0.0/100)

```

(086) IMPDET UNITIS 100 INT IAP: ? (9:00AM; 7-11-1980)

(007984C) (007984D)

£.00000	4956-0
200-0	4956-0
250-0	4956-5
300-0	4955-0
350-0	4955-0
400-0	4955-0
450-0	4955-0
500-0	4955-0
550-0	4955-0
600-0	4955-0
650-0	4955-0
700-0	4955-0
750-0	4955-0
800-0	4955-0
850-0	4955-0
900-0	4955-0
950-0	4955-0
1000-0	4956-0

**REPORT PRODUCTIONS:**

02- 1.00007 001003

INITIAL DEPTN= 1.00+02 METERS

[illegible]

CASE NUMBER: 1

10171744 206410-5.00-01 00601015

[illegible]

3387M 3998°005A -91041 99083 7914191

**RESEARCH IN PROGRESS**

THIS PAGE IS BEST QUALITY PRACTICABLE  
FROM COPY SUBMITTED TO DOD

#	STEP#	STEP#	TYPE#	TYPE#	TYPE#	CTP	AIR	AVGSP
	(M)	(SEC)	(M)	(SEC)	(M)	(M/SEC)	(SEC)	(M/SEC)
1	2.000382+04	1.000187+01	3.153575+03	1.500000+03	2.963917-01	1.485139+03	1.485139+03	1.485139+03
2	5.392742+04	3.030942+01	9.020532+01	1.500000+03	2.963917-01	1.485139+03	1.485139+03	1.485139+03
3	8.097702+04	5.452495+01	3.153588+03	1.500000+03	2.963917-01	1.485139+03	1.485139+03	1.485139+03
4	1.000376+05	7.274446+01	9.021595+01	1.500000+03	2.963917-01	1.485139+03	1.485139+03	1.485139+03

CASE NUMBER: 2  
 INITIAL ANGLE: 1.00+00 DEGREES  
 INITIAL SOUND SPEED: 1509.6+00 M/SEC  
 PROJECTED VECTOR SPEED: 1509.6+00 M/SEC

SUMMARY OF TRAJECTORY:

#	STEP#	STEP#	TYPE#	TYPE#	TYPE#	CTP	AIR	AVGSP
	(M)	(SEC)	(M)	(SEC)	(M)	(M/SEC)	(SEC)	(M/SEC)
1	2.000372+04	1.797124+01	3.163432+03	1.500000+03	2.984156-01	1.485134+03	1.485134+03	1.485134+03
2	5.373410+04	3.010335+01	9.080670+01	1.500000+03	2.984156-01	1.485134+03	1.485134+03	1.485134+03
3	8.078443+04	5.439939+01	3.163429+03	1.500000+03	2.984156-01	1.485139+03	1.485139+03	1.485139+03
4	1.078334+05	7.261343+01	9.081995+01	1.500000+03	2.984156-01	1.485139+03	1.485139+03	1.485139+03

CASE NUMBER: 3  
 INITIAL ANGLE: 1.50+00 DEGREES  
 INITIAL SOUND SPEED: 1509.6+00 M/SEC  
 PROJECTED VECTOR SPEED: 1510.2+00 M/SEC

SUMMARY OF TRAJECTORY:

#	STEP#	STEP#	TYPE#	TYPE#	TYPE#	CTP	AIR	AVGSP
	(M)	(SEC)	(M)	(SEC)	(M)	(M/SEC)	(SEC)	(M/SEC)
1	2.052187+04	1.784407+01	3.179081+03	1.510159+03	3.017608-01	1.485127+03	1.485127+03	1.485127+03
2	5.356446+04	3.007300+01	9.307384+01	1.510159+03	3.017608-01	1.485129+03	1.485129+03	1.485129+03
3	8.060705+04	5.428192+01	3.179091+03	1.510159+03	3.018515-01	1.485131+03	1.485131+03	1.485131+03
4	1.076496+05	7.249080+01	9.367809+01	1.510159+03	3.018515-01	1.485131+03	1.485131+03	1.485131+03

CASE NUMBER: 4  
 INITIAL ANGLE: 2.00+00 DEGREES  
 INITIAL SOUND SPEED: 1509.6+00 M/SEC  
 PROJECTED VECTOR SPEED: 1510.6+00 M/SEC

SUMMARY OF TRAJECTORY:

#	STEP#	STEP#	TYPE#	TYPE#	TYPE#	CTP	AIR	AVGSP
	(M)	(SEC)	(M)	(SEC)	(M)	(M/SEC)	(SEC)	(M/SEC)
1	2.038802+04	1.777545+01	3.202960+03	1.510562+03	3.044308-01	1.485128+03	1.485128+03	1.485128+03
2	5.343107+04	3.590469+01	8.823454+01	1.510562+03	3.044308-01	1.485129+03	1.485129+03	1.485129+03
3	8.047618+04	5.419355+01	3.202978+03	1.510562+03	3.044308-01	1.485132+03	1.485132+03	1.485132+03
4	1.075173+05	7.240316+01	8.821079+01	1.510562+03	3.044308-01	1.485132+03	1.485132+03	1.485132+03

CASE NUMBER: 5  
 INITIAL ANGLE: 2.50+00 DEGREES  
 INITIAL SOUND SPEED: 1509.6+00 M/SEC

THIS PAGE IS BEST QUALITY PRACTICABLE  
 HAVE ONLY FURNISHED TO DDC

PREDICTED VENTED SPEED- 1511.1000 M/SEC

SUMMARY OF TRAJECTORY:

N	STP(EN) (M)	TP(EN) (SEC)	ZTP(EN) (M)	CTP (M/SEC)	JEN (SEC)	AVESP (M/SEC)
1	2.627644+04	1.770901+01	3.232704+03	1.511080+03	3.124176-01	1.485228+03
2	5.343831+04	3.508961+01	6.162643+03	1.511077+03	3.127272-01	1.485236+03
3	8.058948+04	5.427026+01	9.212732+03	1.511081+03	3.127774-01	1.485234+03
4	1.077646+05	7.235093+01	1.162703+04	1.511077+03	3.127785-01	0.000000

CASE NUMBER: 6

INITIAL ANGLE- 3.00+00 DEGREES

INITIAL SOUND SPEED- 1509.4+00 M/SEC

PREDICTED VENTED SPEED- 1511.7+00 M/SEC

SUMMARY OF TRAJECTORY:

N	STP(EN) (M)	TP(EN) (SEC)	ZTP(EN) (M)	CTP (M/SEC)	JEN (SEC)	AVESP (M/SEC)
1	2.422690+04	1.766749+01	3.249128+03	1.511174+03	3.194974-01	1.487851+03
2	5.556632+04	3.739891+01	6.280232+03	1.510392+03	3.219740-01	1.487864+03
3	8.489949+04	5.712638+01	9.264601+03	1.511177+03	3.219535-01	1.487864+03
4	1.162732+05	7.484938+01	1.162732+04	1.510392+03	3.220563-01	0.000000

CASE NUMBER: 7

INITIAL ANGLE- 3.50+00 DEGREES

INITIAL SOUND SPEED- 1509.4+00 M/SEC

PREDICTED VENTED SPEED- 1512.5+00 M/SEC

SUMMARY OF TRAJECTORY:

N	STP(EN) (M)	TP(EN) (SEC)	ZTP(EN) (M)	CTP (M/SEC)	JEN (SEC)	AVESP (M/SEC)
1	2.420363+04	1.765342+01	3.312336+03	1.512643+03	3.282886-01	1.486218+03
2	5.452873+04	3.474827+01	5.960464+03	1.510392+03	3.313977-01	1.486219+03
3	8.296007+04	5.584192+01	9.312690+03	1.512646+03	3.313765-01	1.486221+03
4	1.113371+05	7.493530+01	1.162732+04	1.510392+03	3.315086-01	0.000000

CASE NUMBER: 8

INITIAL ANGLE- 4.00+00 DEGREES

INITIAL SOUND SPEED- 1509.4+00 M/SEC

PREDICTED VENTED SPEED- 1513.3+00 M/SEC

SUMMARY OF TRAJECTORY:

N	STP(EN) (M)	TP(EN) (SEC)	ZTP(EN) (M)	CTP (M/SEC)	JEN (SEC)	AVESP (M/SEC)
1	2.422782+04	1.766902+01	3.362890+03	1.513328+03	3.381973-01	1.485837+03
2	5.419876+04	3.449464+01	5.960464+03	1.510392+03	3.420146-01	1.485839+03
3	8.218964+04	5.531943+01	9.342909+03	1.513330+03	3.420237-01	1.485842+03
4	1.101606+05	7.414443+01	1.162732+04	1.510392+03	3.421698-01	0.000000



CASE NUMBER: 9  
 INITIAL ANGLE= 4.50+00 DEGREES  
 INITIAL SOUND SPEED= 1509.6+00 M/SEC  
 PREDICTED VELOCITY SPEED= 1516.3+00 M/SEC

SUMMARY OF TRAJECTORY:

N	STEP(S)	TYPE(S)	ZP(S)	CTP	A(S)	AVGSP
	(S)	(SEC)	(M)	(M/SEC)	(SEC)	(M/SEC)
1	2.43248+04	1.77187+01	3.42017+03	1.51431+03	3.49449+01	1.48544+03
2	5.40787+04	3.64167+01	5.96064+03	1.51059+03	3.54013+01	1.48544+03
3	8.18333+04	5.51104+01	3.42086+03	1.51431+03	3.53941+01	1.48544+03
4	1.09428+05	7.38059+01	2.98023+03	1.51059+03	3.54248+01	0.00000

CASE NUMBER: 10  
 INITIAL ANGLE= 5.00+00 DEGREES  
 INITIAL SOUND SPEED= 1509.6+00 M/SEC  
 PREDICTED VELOCITY SPEED= 1515.4+00 M/SEC

SUMMARY OF TRAJECTORY:

N	STEP(S)	TYPE(S)	ZP(S)	CTP	A(S)	AVGSP
	(S)	(SEC)	(M)	(M/SEC)	(SEC)	(M/SEC)
1	2.44343+04	1.78057+01	3.48805+03	1.51548+03	3.42083+01	1.48538+03
2	5.41514+04	3.64313+01	5.96064+03	1.51059+03	3.47427+01	1.48538+03
3	8.18487+04	5.51206+01	3.48037+03	1.51542+03	3.47160+01	1.48538+03
4	1.09546+05	7.37780+01	5.96064+03	1.51059+03	3.47424+01	0.00000

CASE NUMBER: 11  
 INITIAL ANGLE= 5.50+00 DEGREES  
 INITIAL SOUND SPEED= 1509.6+00 M/SEC  
 PREDICTED VELOCITY SPEED= 1516.6+00 M/SEC

SUMMARY OF TRAJECTORY:

N	STEP(S)	TYPE(S)	ZP(S)	CTP	A(S)	AVGSP
	(S)	(SEC)	(M)	(M/SEC)	(SEC)	(M/SEC)
1	2.46320+04	1.79361+01	3.50167+03	1.51662+03	3.76093+01	1.48543+03
2	5.44037+04	3.64295+01	7.45081+03	1.51059+03	3.82396+01	1.48548+03
3	8.21782+04	5.53248+01	3.50908+03	1.51465+03	3.81721+01	1.48538+03
4	1.09952+05	7.40198+01	5.96064+03	1.51059+03	3.82483+01	0.00000

CASE NUMBER: 12  
 INITIAL ANGLE= 6.00+00 DEGREES  
 INITIAL SOUND SPEED= 1509.6+00 M/SEC  
 PREDICTED VELOCITY SPEED= 1518.6+00 M/SEC

SUMMARY OF TRAJECTORY:

N	STEP(S)	TYPE(S)	ZP(S)	CTP	A(S)	AVGSP
	(S)	(SEC)	(M)	(M/SEC)	(SEC)	(M/SEC)
1	2.49087+04	1.81185+01	3.64316+03	1.51795+03	3.91597+01	1.48526+03
2	5.48457+04	3.69204+01	5.96064+03	1.51059+03	3.98371+01	1.48532+03
3	8.27646+04	5.57244+01	3.64258+03	1.51797+03	3.97809+01	1.48534+03

4 1.107235-05 7.452780-01 2.980232-08 1.510392-03 3.987426-01 0.000000

CASE NUMBER: 13  
INITIAL ANGLES- 0.50-00 DEG/SEC  
INITIAL SOUND SPEED- 1509.4-06 M/SEC  
PREDICTED WATER SPEED- 1519.4-00 M/SEC

SUMMARY OF TRAJECTORY:

E	STP (m)	TTP (m)	ZTP (m)	CTP (m/SEC)	J (SEC)	AVGSP (M/SEC)
1	2.720314-04	1.834504-01	3.213400-03	1.510400-03	4.004403-01	1.400149-03
2	5.550280-04	3.753350-01	3.225200-00	1.510392-03	4.164387-01	1.400161-03
3	8.373116-04	5.634764-01	3.735040-03	1.510445-03	4.153763-01	1.400164-03
4	1.110500-05	7.534124-01	5.960444-00	1.510392-03	4.164510-01	0.000000

CASE NUMBER: 14  
INITIAL ANGLES- 7.00-00 DEG/SEC  
INITIAL SOUND SPEED- 1509.4-06 M/SEC  
PREDICTED WATER SPEED- 1521.6-00 M/SEC

SUMMARY OF TRAJECTORY:

E	STP (m)	TTP (m)	ZTP (m)	CTP (m/SEC)	J (SEC)	AVGSP (M/SEC)
1	2.778430-04	1.869473-01	3.836912-03	1.520079-03	4.273430-01	1.400645-03
2	5.442957-04	3.794315-01	5.960444-00	1.520392-03	4.354244-01	1.400651-03
3	8.507849-04	5.723301-01	3.817703-03	1.520091-03	4.345107-01	1.400655-03
4	1.132270-05	7.630490-01	5.960444-00	1.510392-03	4.350013-01	0.000000

CASE NUMBER: 15  
INITIAL ANGLES- 7.50-00 DEG/SEC  
INITIAL SOUND SPEED- 1509.4-06 M/SEC  
PREDICTED WATER SPEED- 1522.7-00 M/SEC

SUMMARY OF TRAJECTORY:

E	STP (m)	TTP (m)	ZTP (m)	CTP (m/SEC)	J (SEC)	AVGSP (M/SEC)
1	2.844094-04	1.913934-01	3.934112-03	1.522000-03	4.470307-01	1.407363-03
2	5.779647-04	3.801005-01	2.980232-00	1.510392-03	4.569604-01	1.407387-03
3	8.490285-04	5.849100-01	3.934958-03	1.522700-03	4.557374-01	1.407391-03
4	1.162672-05	7.817350-01	1.920933-07	1.510392-03	4.569643-01	0.000000

CASE NUMBER: 16  
INITIAL ANGLES- 8.00-00 DEG/SEC  
INITIAL SOUND SPEED- 1509.4-06 M/SEC  
PREDICTED WATER SPEED- 1524.5-00 M/SEC

SUMMARY OF TRAJECTORY:

E	STP (m)	TTP (m)	ZTP (m)	CTP (m/SEC)	J (SEC)	AVGSP (M/SEC)
1	2.844094-04	1.913934-01	3.934112-03	1.522000-03	4.470307-01	1.407363-03
2	5.779647-04	3.801005-01	2.980232-00	1.510392-03	4.569604-01	1.407387-03
3	8.490285-04	5.849100-01	3.934958-03	1.522700-03	4.557374-01	1.407391-03
4	1.162672-05	7.817350-01	1.920933-07	1.510392-03	4.569643-01	0.000000

1 2.940026+04 1.973585+01 4.000000+03 1.324477+03 4.783791-01 1.408405+03  
 2 5.954278+04 4.000708+01 5.940444-00 1.510392+03 4.799268-01 1.408421+03  
 3 8.969092+04 4.024650+01 4.090672+03 1.524499+03 4.788124-01 1.408424+03  
 4 1.100315+05 8.032591+01 3.940644-00 1.510392+03 4.861010-01 0.000000

CASE NUMBER: 17  
 INITIAL ANGLES- 0.50+00 0160883  
 INITIAL SOUND SPEED- 1500.4+00 M/SEC  
 PREDICTED WATER SPEED- 1520.4+00 M/SEC

SUMMARY OF TRAJECTORY:

E	ATP (m)	TP (sec)	ZTP (m)	CIP (m/SEC)	J (sec)	AVGSP (m/SEC)
1	3.078909+04	2.044645+01	4.240002+03	1.520409+03	4.953225-01	1.409049+03
2	6.227345+04	4.179740+01	1.192093-07	1.510392+03	5.051328-01	1.409044+03
3	9.374875+04	6.293357+01	4.250181+03	1.520422+03	5.045828-01	1.409049+03
4	1.253066+05	8.407309+01	1.192093-07	1.510392+03	5.054470-01	0.000000

CASE NUMBER: 18  
 INITIAL ANGLES- 0.00+00 0160883  
 INITIAL SOUND SPEED- 1500.4+00 M/SEC  
 PREDICTED WATER SPEED- 1520.5+00 M/SEC

SUMMARY OF TRAJECTORY:

E	ATP (m)	TP (sec)	ZTP (m)	CIP (m/SEC)	J (sec)	AVGSP (m/SEC)
1	3.314372+04	2.220779+01	4.430972+03	1.520400+03	5.233321-01	1.402442+03
2	6.403972+04	4.403217+01	3.940644-00	1.510392+03	5.343961-01	1.402509+03
3	1.007787+05	6.752674+01	4.434099+03	1.520400+03	5.320334-01	1.402514+03
4	1.340177+05	9.019722+01	2.900232-00	1.510392+03	5.350544-01	0.000000

CASE NUMBER: 19  
 INITIAL ANGLES- 0.50+00 0160883  
 INITIAL SOUND SPEED- 1500.4+00 M/SEC  
 PREDICTED WATER SPEED- 1530.4+00 M/SEC

SUMMARY OF TRAJECTORY:

E	ATP (m)	TP (sec)	ZTP (m)	CIP (m/SEC)	J (sec)	AVGSP (m/SEC)
1	3.954027+04	2.438900+01	4.744037+03	1.530433+03	5.543983-01	1.408253+03
2	7.049583+04	5.319054+01	1.192093-07	1.510392+03	5.670945-01	1.408269+03
3	1.190438+05	8.000912+01	4.745250+03	1.530433+03	5.669800-01	1.408271+03
4	1.600316+05	1.008096+02	3.940644-00	1.510392+03	5.682490-01	0.000000

CASE NUMBER: 20  
 INITIAL ANGLES- 0.00+01 0160883  
 INITIAL SOUND SPEED- 1500.4+00 M/SEC  
 PREDICTED WATER SPEED- 1532.4+00 M/SEC

DAY DEPTH EXCEEDS DEPTH LIMIT: 2.000000+04 METERS



## REFERENCES

1. D. E. Weston, Proc. Phys. Soc. (London) 73, 365-384 (1958).
2. R. C. Shockley, J. Acoust. Soc. Am. (to be published).
3. L. D. Landau and E. M. Lifshitz, *Mechanics*, Pergamon Press, Reading, Mass. pp 154-158 (1960).
4. D. M. Milder, J. Acoust. Soc. Am. 46, pp 1259-1263 (1969).
5. Byrd, PF and Friedman, MD, *Handbook of Elliptic Integrals for Engineers and Scientists*, Springer-Verlag, New York (1971).
6. Mathpac Univac Corporation. SPLN1 and SPLN2 are documented in a number of manuals covering resident subroutines.

INITIAL DISTRIBUTION LIST

DEFENSE ADVANCED RESEARCH PROJECTS AGENCY  
DR. G. GUSTAFSON

ARPA RESEARCH CENTER  
MOFFETT FIELD, CA  
R. TRUEBLOOD

NAVAL ELECTRONIC SYSTEMS COMMAND  
PME-124 (CAPT H. COX)  
PME-124/60 (DR. G. HETLAND)  
NELEX-320 (CDR D. GRIFFITH)

NAVAL RESEARCH LABORATORY  
DR. B. ADAMS  
H. BROCK  
DR. B. HURDLE  
DR. R. FERRIS  
D. NUTILE  
A. GUTHRIE

NEW LONDON LABORATORY  
NAVAL UNDERWATER SYSTEMS CENTER  
CODE 314 (DR. H. WEINBERG)  
CODE 312 (DR. F. DI NAPOLI)

THE UNIVERSITY OF TEXAS  
APPLIED RESEARCH LABORATORY  
P.O. BOX 8029  
AUSTIN, TX 78712  
DR. L. HAMPTON  
DR. S. MITCHELL

BOLT BERANEK AND NEWMAN, INC.  
50 MOULTON STREET  
CAMBRIDGE, MA 02138  
DR. P. W. SMITH

INSTITUTE FOR ACOUSTICAL RESEARCH  
615 S.W. 2ND AVENUE  
MIAMI, FL 33130  
DR. W. JOBST  
L. DOMINIJANNI

OCEAN DATA SYSTEMS, INC.  
3581 KENYON STREET  
SAN DIEGO, CA 92110  
K. OSBORNE  
DR. F. RYAN  
DR. J. CROUCH

SCIENCE APPLICATIONS, INC.  
8400 WESTPARK DRIVE  
MC LEAN, VA 22101  
C. SPOFFARD

DEFENSE DOCUMENTATION CENTER (12)